

Low temperature electronic properties of Sr₂RuO₄ II: Superconductivity

Ralph Werner

*Physics Department, Brookhaven National Laboratory, Upton, NY 11973-5000, USA and
Institut für Theorie der Kondensierten Materie, Universität Karlsruhe, 76128 Karlsruhe, Germany
(November 9, 2018)*

Preprint. Typeset using REVTeX.

The body centered tetragonal structure of Sr₂RuO₄ gives rise to umklapp scattering enhanced inter-plane pair correlations in the d_{yz} and d_{zx} orbitals. Based on symmetry arguments, Hund's rule coupling, and a bosonized description of the in-plane electron correlations the superconducting order parameter is found to be a orbital-singlet spin-triplet with two spatial components. The spatial anisotropy is 7%. The different components of the order parameter give rise to two-dimensional gapless fluctuations. The phase transition is of third order. The temperature dependence of the pair density, specific heat, NQR, Knight shift, and susceptibility are in agreement with experimental results.

I. INTRODUCTION

Sr₂RuO₄ has quickly triggered a large interest because of its structural similarity to the cuprates and the unconventional superconductivity below $T_c \sim 1$ K.¹ The material is tetragonal at all temperatures.² The three bands cutting the Fermi level with quasi two-dimensional Fermi surfaces^{3,4} can be mainly associated with the three t_{2g} orbitals of the Ru⁴⁺ ions.^{5,6} The transport is Fermi liquid like for $T_c < T < 30$ K⁷⁻⁹ and strongly anisotropic along the c axis.¹ The enhanced specific heat, magnetic susceptibility and electronic mass indicate the presence of significant correlations.^{1,4,10}

The superconducting order parameter was proposed to have p -wave symmetry analogous to superfluid ³He.^{11,12} This was supported by magnetic experimental probes,¹³⁻¹⁶ but has not been proven unambiguously in spite of large efforts in Andreev spectroscopy,^{17,18} thermal conductivity,¹⁹⁻²² and ac-susceptibility²³ measurements. No indication for ferromagnetic correlations has been found.²⁴⁻²⁷ The specific heat,²⁸⁻³⁰ thermal conductivity,³¹ and nuclear quadrupole resonance (NQR)⁹ are consistent with two-dimensional gapless fluctuations in the superconducting phase. For a more detailed overview see Refs. 6,32-34.

The present paper is part II of a series of three. In part I (Ref. 32) the quasi one-dimensionality of the kinetic energy of the d_{zx} and d_{yz} electrons has been used to derive a bosonized effective model. At intermediate coupling the interaction leads to a quasi one-

dimensional model for the magnetic degrees of freedom. The resulting spectrum of elementary excitations allows for the coherent description of the observed enhanced dynamical magnetic susceptibility²⁴ including the observed scale invariance.³⁵ Together with the two-dimensional correlations the normal state effective mass renormalization,^{36,37} the specific heat coefficient²⁸⁻³⁰ and the static magnetic susceptibility enhancements^{1,7,10} can be described consistently.

This work is devoted to the superconducting phase. The phase transition to the superconducting state in Sr₂RuO₄ is three dimensional and the specific heat has a shape that is similar to that of a mean-field transition at the transition temperature.^{28,30} The low temperature specific heat data are clearly inconsistent with the BCS theory.^{38,39} This scenario suggests the combination of a mean-field induced three-dimensional transition (Sec. II) with electronic correlations dominated by the quasi two-dimensional configuration (Sec. III). Similar approaches have been successfully applied to coupled spin chains.⁴⁰ The model consistently can account for the experimental data concerning the temperature dependence of the pair density, specific heat, susceptibility and thermal conductivity (Sec. IV). A detailed comparison of the present approach with the p -wave picture is given (Sec. V).

Part III (Ref. 41) consistently explains the experimentally observed unconventional transitions under magnetic fields in terms of the model derived here.

II. MEAN-FIELD APPROACH

The generic model Hamiltonian is

$$H = \sum_{\substack{\mathbf{l}, \mathbf{l}' \\ \nu, \nu', \sigma}} t_{\mathbf{l}, \mathbf{l}'}^{\nu, \nu'} c_{\mathbf{l}, \nu, \sigma}^\dagger c_{\mathbf{l}', \nu', \sigma} + \sum_{\substack{\mathbf{l}, \nu, \sigma \\ \nu', \sigma'}} U_{\sigma, \sigma'}^{\nu, \nu'} n_{\mathbf{l}, \nu, \sigma} n_{\mathbf{l}, \nu', \sigma'}. \quad (1)$$

In this notation the electron creation and annihilation operators are $c_{\mathbf{l}, \nu, \sigma}^\dagger$ and $c_{\mathbf{l}, \nu, \sigma}$ for orbital ν with spin σ on site \mathbf{l} , $n_{\mathbf{l}, \nu, \sigma}$ is the usual electronic density operator, $t_{\mathbf{l}, \mathbf{l}'}^{\nu, \nu'}$ is the hopping matrix element. The intra-orbital Coulomb repulsion is larger than the inter-orbital repulsion, i.e., $U_{\sigma \neq \sigma'}^{\nu = \nu'} = U_0 > U_1 = U_{\sigma \neq \sigma'}^{\nu \neq \nu'}$ and $U_0 > U_2 = U_{\sigma = \sigma'}^{\nu \neq \nu'}$. The Hamiltonian in Eq. (1) is quasi two-dimensional.³²

The correlations in effective one-dimensional systems show power law behavior.⁴² They are always more singular than two-dimensional correlations which diverge at

most logarithmically.⁴³ Since the kinetic energy of the d_{zx} and d_{yz} electrons is quasi one-dimensional we expect their correlations to play a dominant role.³²

In order for the system to undergo a finite temperature phase transition the coupling of the RuO₂ planes is necessary.⁴⁴ The inter-plane $d_{z\nu}$ - $d_{z\nu}$ hopping has been estimated in Ref. 32 to be $t_{\perp} \approx 0.02$ eV and is an order of magnitude smaller than the in-plane hopping. The inter-plane hopping involving d_{xy} orbitals is expected to be significantly smaller for geometry reasons.⁶ It follows that the $d_{z\nu}$ - $d_{z\nu}$ subsystem should drive the transition. This conclusion is in contrast to most other approaches^{6,38,45-48} which assume the pair correlations of the d_{xy} electrons to be dominant.

The sensitivity of the superconducting instability on the dimensionality can be probed by experiments under pressure. Recent ultrasonic measurements⁴⁹ suggest that the superconducting T_c increases upon uniaxial pressure along the crystallographic c axis. This is reminiscent of an increase in the inter-plane coupling and is consistent with a pairing mechanism induced by inter-plane pair correlations as proposed by Baskaran.¹²

On the other hand T_c has been shown to decrease under hydrostatic pressure.^{50,37} This can be understood in terms of the decrease of the in-plane lattice parameter which in turn increases the in-plane hopping parameters which lowers the relative interaction strength and renders the $d_{z\nu}$ - $d_{z\nu}$ subsystem more two-dimensional. It can thus be concluded that hydrostatic pressure lowers the in-plane correlations³² including those of Coopers pairs leading to a lower T_c . Note that this assumption finds strong support in the decrease of the effective thermodynamic electronic masses under hydrostatic pressure observed in dHvA measurements.³⁷

A. Normal phase instability

In summary the discussion above suggests the presence of an inter-plane pair-correlation term between the planar $d_{z\nu}$ - $d_{z\nu}$ subsystems driving the observed phase transition. Such a term can be written in form of the lowest order coherent inter-plane pair-hopping term:

$$H_p = \sum_{\substack{\nu, \mu, \sigma \\ \nu', \mu', \sigma'}} V_p^{\mu, \mu'} \sum_{\langle \mathbf{l}, \mathbf{l}' \rangle} c_{\mathbf{l}, \mu, \sigma}^{\dagger} c_{\mathbf{l}', \nu, \sigma} c_{\mathbf{l}, \mu', \sigma'}^{\dagger} c_{\mathbf{l}', \nu', \sigma'}. \quad (2)$$

The orbital indices $\nu, \mu, \nu', \mu' \in \{x, y\}$ are restricted by the Pauli principle for $\sigma' = \sigma$ to $\mu' \neq \mu$ and $\nu' \neq \nu$. The second sum runs over nearest-neighbor sites where \mathbf{l} and \mathbf{l}' are on neighboring planes.

Note that such an inter-plane pair-correlation term may have different origins. Possible suggestions are Coulomb interactions screened on the scale of the inter-plane distance $c/2$ or electron-phonon interaction where the phonon degrees of freedom⁵¹ have been integrated out. Since a discussion of the specific origin of the term

would not be conclusive in the context of the present approach it is omitted.

Instead, a phenomenological estimate for the pair-hopping amplitude can be obtained by requiring its value to be consistent with the single particle inter-plane hopping t_{\perp} , i.e., $V_p^{\mu, \mu'} \sim t_{\perp}^2/v_F$. The energy denominator is estimated by a typical in-plane energy scale. Here the kinetic scale v_F was chosen for the sake of definiteness. Depending on the specific mechanism, an interaction energy scale $U_{\sigma, \sigma'}^{\mu, \mu'}$ as the energy denominator is also conceivable. Since the system has been shown to be in the intermediate coupling³² regime, i.e., $v_F \sim U_{\sigma, \sigma'}^{\mu, \mu'}$, the numerical outcome is similar. Considering that $t_{\perp} \approx 0.02$ eV³² and $v_F = \bar{v}_F/a \approx 0.7$ eV²⁷ one has $t_{\perp}^2/v_F \approx 6$ K $\ll v_F$ suggesting that a mean-field decoupling of Eq. 2 is reasonable.

Fourier transforming the Fermi operators in Eq. (2) leads to the Hamiltonian

$$H_p = \sum_{\substack{\nu, \mu, \sigma \\ \nu', \mu', \sigma'}} \sum_{\mathbf{k}, \mathbf{k}', \mathbf{q}} \frac{V_{\mathbf{q}}}{N} c_{\mathbf{k}, \mu, \sigma}^{\dagger} c_{\mathbf{q}-\mathbf{k}, \mu', \sigma'}^{\dagger} c_{\mathbf{q}-\mathbf{k}', \nu', \sigma'} c_{\mathbf{k}', \nu, \sigma} \quad (3)$$

with the effective Potentials

$$V_{\mathbf{q}} \approx \frac{t_{\perp}^2}{v_F} \cos \frac{a}{2} q_x \cos \frac{a}{2} q_y \cos \frac{c}{2} q_z. \quad (4)$$

For $\mathbf{q} = \mathbf{q}_j$ with

$$\mathbf{q}_j \in \left\{ \left(\frac{2\pi}{a}, \frac{2\pi}{a}, \frac{2\pi}{c} \right)^{\dagger}, \frac{2\pi}{a} \hat{x}, \frac{2\pi}{a} \hat{y}, \frac{2\pi}{c} \hat{z} \right\} \quad (5)$$

the potential is extremal and attractive, i.e., $V_{\mathbf{q}_j} \approx -t_{\perp}^2/v_F < 0$. As a consequence of the body centered tetragonal lattice structure the \mathbf{q}_j are reciprocal lattice vectors. In other words, the body centered tetragonal lattice symmetry allows for an unklapp scattering driven pair instability.

Within the configuration space of the d_{zx} - d_{yz} subsystem six possible pairing states can be found. There is an “equal-flavor” doublet which can be identified as a spin-singlet

$$P_{0, \pm}(\mathbf{q}) = \sum_{\mathbf{k}} \left(c_{\mathbf{q}-\mathbf{k}, x, \uparrow} c_{\mathbf{k}, x, \downarrow} \pm c_{\mathbf{q}-\mathbf{k}, y, \uparrow} c_{\mathbf{k}, y, \downarrow} \right), \quad (6)$$

as well as a “mixed-flavor” doublet with a spin-singlet and a $S^z = 0$ spin-triplet component

$$P_{1, \pm}(\mathbf{q}) = \sum_{\mathbf{k}} \left(c_{\mathbf{q}-\mathbf{k}, x, \uparrow} c_{\mathbf{k}, y, \downarrow} \pm c_{\mathbf{q}-\mathbf{k}, x, \downarrow} c_{\mathbf{k}, y, \uparrow} \right). \quad (7)$$

The “mixed-flavor” doublet with spin-triplet components with magnetization quantum number $|S^z| = 1$ is

$$P_{2, \pm}(\mathbf{q}) = \sum_{\mathbf{k}} \left(c_{\mathbf{q}-\mathbf{k}, x, \uparrow} c_{\mathbf{k}, y, \uparrow} \pm c_{\mathbf{q}-\mathbf{k}, x, \downarrow} c_{\mathbf{k}, y, \downarrow} \right). \quad (8)$$

The six components can be regrouped³⁴ as an orbital-triplet spin-singlet

$$\mathbf{P}_s^{t\dagger} = \left(P_{0,+}^\dagger, P_{0,-}^\dagger, P_{1,-}^\dagger \right) \quad (9)$$

and an orbital-singlet spin-triplet

$$\mathbf{P}_t^{s\dagger} = \left(P_{2,+}^\dagger, P_{2,-}^\dagger, P_{1,+}^\dagger \right) \quad (10)$$

given here in vectorial representation.⁵² The pair operator components have a very similar structure as the p -wave components initially discussed by Rice and Sigrist.¹¹ Notably, the $P_{2,\pm}$ components have the same spin-structure as the unitary state with E_u symmetry proposed in the p -wave scenario for Sr_2RuO_4 .⁵³ The degrees of freedom form a two-dimensional analog to those of the A phase^{54,55} of ^3He . The crucial difference is that all components $P_{a,\pm}$ render even parity real-space wavefunctions because the antisymmetry of the total electronic wavefunction is established through either the spin-singlet or the orbital-singlet configuration. A closer account of the resulting symmetries is given separately in Ref. 34.

Introducing the variables $a \in \{0, 1, 2\}$ and $b \in \{+, -\}$ and switching to time-dependent pair operators in the Heisenberg representation the bare pair susceptibilities are

$$\chi_{a,b}^{(P)}(\mathbf{q}, \omega) = \langle P_{a,b}(\mathbf{q}, \omega) P_{a,b}^\dagger(\mathbf{q}, \omega) \rangle. \quad (11)$$

The random phase approximation (RPA) is equivalent in its static limit to the mean-field approximation. The RPA pair susceptibility is

$$\chi_P(\mathbf{q}, \omega) = \frac{1}{4} \sum_{a,b} \frac{\chi_{a,b}^{(P)}(\mathbf{q}, \omega)}{1 + V_{\mathbf{q}} \chi_{a,b}^{(P)}(\mathbf{q}, \omega)}. \quad (12)$$

The mean-field phase transition occurs at $T = T_c$ when the Stoner criterion $\chi_{a,b}^{(P)}(\mathbf{q}_j, 0)|_{T_c} = \chi_{a,b}^{(P)}(0, 0)|_{T_c} = -V_{\mathbf{q}_j}^{-1} = V_0^{-1}$ is fulfilled. The estimated value of $V_0 \approx 6$ K is consistent with the low critical temperature of $T_c = 1.5$ K.

In order to make a quantitative prediction of T_c the $\chi_{a,b}^{(P)}(0, 0)$ have to be determined as a function of temperature within the effectively two-dimensional model based on Eq. (1). This is not straightforward as becomes clear from the discussions in Ref. 32 and is left to future studies.

Mean-field approaches do not allow to control rigorously the local constraint imposed by the Pauli exclusion principle.⁵⁶ Since the filling factors of the orbitals²⁷ are $n_\mu \sim 1.3$ it is important in a mean-field approach to include effects of the Pauli exclusion principle at least in an approximate manner. Formally this can be achieved by introducing a phenomenological orbital-

dependent weighing factor g_a^2 of order one in the denominator of Eq. (12):

$$\left[1 + V_{\mathbf{q}} \chi_{a,b}^{(P)}(\mathbf{q}, \omega) \right]^{-1} \rightarrow \left[1 + g_a^2 V_{\mathbf{q}} \chi_{a,b}^{(P)}(\mathbf{q}, \omega) \right]^{-1}. \quad (13)$$

The pair-hopping process in Eq. (2) with $\mu = \mu'$, i.e., $a = 0$ in Eq. (13), requires the orbital μ to be unoccupied in the initial state which is very unlikely with $n_\mu \sim 1.3$. Pair-hopping processes with $\mu \neq \mu'$ in Eq. (2), where $a = 1$ or $a = 2$ in Eq. (13), are much less effected by the Pauli exclusion principle. Consequently $g_0^2 \ll g_1^2 \approx g_2^2 \sim 1$ and the phase transition occurs in the mixed flavor channels.⁵⁷ This conclusion is only altered if the in-plane equal-flavor-doublet correlations $\chi_{0,b}^{(P)}(\mathbf{q}, \omega)$ are much larger than those of the mixed-flavor sector for which there is no indication to be found.

In the presence of Hund's rule coupling the spin-triplet energy expectation values are always smaller than those of the spin-singlet.¹²

$$|\langle \mathbf{P}_t^{s\dagger} | H | \mathbf{P}_t^{s\dagger} \rangle| < |\langle \mathbf{P}_t^{t\dagger} | H | \mathbf{P}_t^{t\dagger} \rangle| \quad (14)$$

Consequently $\langle P_{0,+}^\dagger \rangle = \langle P_{0,-}^\dagger \rangle = \langle P_{1,-}^\dagger \rangle = 0$. Consistent with $S = 1$ moments on Ru^{4+} impurities in Sr_2IrO_4 ,⁵⁸ one finds mixed-orbital spin-triplet pairing or, equivalently, orbital-singlet spin-triplet pairing. The initial $\text{SU}(2) \otimes \text{SU}(2)$ symmetry of the two electron spins is broken down to $\text{SO}(3)$. The order parameter carries spin one and explains the absence of a change of the Knight shift¹⁴ and of the magnetic susceptibility¹⁵ in the superconducting phase.

At this point it is important to notice that the estimated value for Hund's rule coupling⁵⁹ in Sr_2RuO_4 of $J_H \approx 0.2 - 0.4$ eV is larger than the estimate for the spin-orbit coupling⁶⁰ of $\lambda \approx 0.1$ eV. Consequently orbital-singlet pairing is possible even if the degeneracy of the d_{zx} and d_{yz} orbitals is lifted due to spin-orbit coupling because the larger Hund's rule coupling over-compensates the effect.

B. Comment on competing energies

Since in the context of the superconducting cuprates it has become habitual to discuss the pair instability in terms of the competition between kinetic and potential energies⁶¹ it is useful here to clarify the situation in the present approach to Sr_2RuO_4 .

In the superconducting state of a BCS superconductor the single particle excitations are gapped and hence the system loses kinetic energy in all spatial directions. The loss is over-compensated by the gain in condensation energy. The intuitive idea is that the system gains "potential energy" through the attractive potential mediated by the phonons.

Here the situation is similar, the system loses kinetic energy both in-plane as well as out-of-plane. In the light of the two-dimensionality of the band structure⁶ the loss of kinetic energy in the RuO₂ planes is at least an order of magnitude larger than that along the *c* axis. The gain in pair hopping energy that one might anticipate through the inter-plane coupling term Eq. (2) is quite small—unlike the case discussed⁶² in the superconducting cuprates.

Instead, the gain in condensation energy overcompensates the loss of kinetic energy as becomes obvious from the sine-Gordon model onto which part of the degrees of freedom in Sr₂RuO₄ are mapped in Sec. III D: the ground state energy is lowered proportional to a given power of the gap *even though* the single particle excitations are gapped [c.f. Eq. 55 and Ref. 63]. Or, viewed from the perspective of the collective condensation, the ground state energy is lowered *because* the single particle excitations are gapped.

Moreover, the notion of potential and kinetic energy is obscured in the bosonized approach introduced in Ref. 32 and applied here in Sec. III. Notably in the one-dimensional limit with preserved SU(2) invariance the Bose fields and their dual fields are equivalent^{64–66} and so are kinetic and potential energy. In this light the discrimination between the two appears obsolete and the energy gain is explained most naturally simply by the condensation of the electrons in the collective state below the gap.

C. Superconducting phase

The order parameter is a spin-one SO(3) triplet with components $\langle P_{t,\nu}^s \rangle \neq 0$. Together with the global phase degree of freedom this implies that the order parameter has SO(3)⊗SO(2) symmetry.

These results are consistent with the implications from the bosonized microscopic model of the in-plane correlations discussed in Sec. III. There it will be shown that there are two degenerate saddle points with slightly different spatial anisotropies. This leads to a total SO(3)⊗SO(2)⊗SO(2) symmetry of the order parameter. The thermodynamic implications of the resulting gapless modes of the order parameter are discussed in detail in Sec. III E.

The usual mean-field decoupling of the pair operators is

$$\mathbf{P}_t^{s\dagger} \mathbf{P}_t^s \approx \mathbf{P}_t^{s\dagger} \langle \mathbf{P}_t^s \rangle + \mathbf{P}_t^s \langle \mathbf{P}_t^s \rangle^* - |\langle \mathbf{P}_t^s \rangle|^2. \quad (15)$$

The mean-field decoupling Eq. (15) has to be applied to the inter-plane Hamiltonian Eq. (2). The mean-field contribution $H_{\text{mf}} \approx H_{\perp}$ is

$$H_{\text{mf}} = V_0 \sum_{\mathbf{l}} \left[2 \text{Re} \mathbf{P}_t^{s\dagger}(\mathbf{l}) \langle \mathbf{P}_t^s \rangle - \left| \langle \mathbf{P}_t^s \rangle \right|^2 \right]. \quad (16)$$

The total Hamiltonian $H + H_{\text{mf}}$ usually permits a Landau expansion of the free energy of the system. This is done in Sec. III F consistent with the bosonized microscopic model for the in-plane correlations to allow for a more quantitative analysis.

An important critique of the orbital-singlet pairing mechanism is that in the *absence of interaction* electrons can only pair where the idealized, one-dimensional bands of the d_{zx} and d_{yz} orbitals cross in reciprocal space. The resulting pairing phase space is much too small to account for the specific heat anomaly at the phase transition [c.f. Sec. IV B]. At *intermediate coupling*, as relevant for Sr₂RuO₄,³² interaction effects significantly enhance the pairing phase space. A close discussion is given in Ref. 34 where it is shown that the interactions lead to a rather homogeneous gap function. See also Sec. III F.

D. γ sheet: inter-band proximity effect

The coupling of the different bands through the inter-band proximity effect and the resulting single transition temperature for all electronic degrees of freedom has been discussed in earlier work.^{6,38,46} In the present model the driving correlations are those of the d_{zx} and d_{yz} electrons as a result of the geometrically strongly enhanced inter-plane coupling of with respect to the d_{xy} electrons.^{6,32}

To obtain a qualitative theoretical picture including the d_{xy} orbitals one must consider the terms in the full Hamiltonian Eq. (1) that are left out of the d_{zx} - d_{yz} Hamiltonian Eqs. (19) and (23) discussed in Sec. III.

$$H_{\gamma} = \sum_{\mathbf{l}, \mathbf{l}', \sigma} t_{\mathbf{l}, \mathbf{l}'}^{\gamma, \gamma} c_{\mathbf{l}, \gamma, \sigma}^{\dagger} c_{\mathbf{l}', \sigma} + \sum_{\mathbf{l}, \sigma} U_0^{\gamma} n_{\mathbf{l}, \gamma, \uparrow} n_{\mathbf{l}, \gamma, \downarrow} + \sum_{\substack{\mathbf{l}, \sigma \\ \nu \neq \gamma}} (U_1^{\gamma} n_{\mathbf{l}, \gamma, \sigma} n_{\mathbf{l}, \nu, \sigma' \neq \sigma} + U_2^{\gamma} n_{\mathbf{l}, \gamma, \sigma} n_{\mathbf{l}, \nu, \sigma}) \quad (17)$$

The hopping parameters were given in Ref. 32 as $t_{\mathbf{l}, \mathbf{l}}^{\gamma, \gamma} = -0.39$ eV, $t_{\mathbf{l}, \mathbf{l}+\hat{x}}^{\gamma, \gamma} = t_{\mathbf{l}, \mathbf{l}+\hat{y}}^{\gamma, \gamma} = -0.27$ eV, and $t_{\mathbf{l}, \mathbf{l}+\hat{x}+\hat{y}}^{\gamma, \gamma} = -0.11$ eV. From the symmetry of the t_{2g} orbitals⁶ follows that in lowest order the interaction parameters U_0^{γ} , U_1^{γ} , and U_2^{γ} are similar to those introduced in Ref. 32 in the context of the d_{zx} - d_{yz} subsystem and are thus smaller but of the similar magnitude as v_{F} .

The inter-orbital terms $\sim U_1^{\gamma}$ and $\sim U_2^{\gamma}$ can formally be mean-field decoupled via

$$n_{\mathbf{l}, \gamma, \sigma} n_{\mathbf{l}, \nu, \sigma'} \approx \langle c_{\mathbf{l}, \gamma, \sigma}^{\dagger} c_{\mathbf{l}, \nu, \sigma'}^{\dagger} \rangle c_{\mathbf{l}, \gamma, \sigma} c_{\mathbf{l}, \nu, \sigma'} + \langle c_{\mathbf{l}, \gamma, \sigma} c_{\mathbf{l}, \nu, \sigma'} \rangle c_{\mathbf{l}, \gamma, \sigma}^{\dagger} c_{\mathbf{l}, \nu, \sigma'}^{\dagger} - \langle c_{\mathbf{l}, \gamma, \sigma}^{\dagger} c_{\mathbf{l}, \nu, \sigma'}^{\dagger} \rangle \langle c_{\mathbf{l}, \gamma, \sigma} c_{\mathbf{l}, \nu, \sigma'} \rangle. \quad (18)$$

The mean-field contributions $\langle c_{\mathbf{l}, \gamma, \sigma} c_{\mathbf{l}, \nu, \sigma'} \rangle$ couple the d_{xy} electrons directly to the pair instability driven by the correlations in the d_{zx} and d_{yz} bands and induce pairs in the γ band. There is only one phase transition.

Since the inter-band proximity effect is usually strong³⁸ a single gap is assumed herein. It has been argued that Sr₂RuO₄ might represent a particular case where the inter-band proximity effect is suppressed⁴⁵ leading to a double gap⁴⁷ structure. No signature of a second gap has been observed in point contact¹⁷ or thermal conductivity experiments³¹ though.

In principle the inter-plane pair hopping term Eq. (2) must be extended to include the d_{xy} or γ orbitals, i.e., $\nu, \mu, \nu', \mu' \in \{x, y, \gamma\}$ as well as the free energy Eq. (58). Since from the orbital geometry $g_{\gamma, \gamma} \ll g_{\gamma, x} = g_{\gamma, y} \ll g_{x, y}$ those contributions are small so they will only contribute small quantitative corrections.

III. MICROSCOPIC IN-PLANE MODEL

The microscopic model derived for the d_{zx} - d_{yz} subsystem in Ref. 32 successfully has been applied to describe the normal state properties in Sr₂RuO₄. Consequently it is reasonable to adapt the same approach for the in-plane correlations to describe the superconducting properties. To assure consistency in the notation of the present manuscript the elementary results are given in the following. Please refer to Ref. 32 for the details.

As discussed in Sec. II the relevant correlations are those of the electrons in the d_{zx} and d_{yz} orbitals. The dominant hopping amplitudes are quasi one-dimensional and given by $t_0 = t_{\mathbf{l}, \mathbf{l}+\hat{x}}^{x, x} = t_{\mathbf{l}, \mathbf{l}+\hat{y}}^{y, y}$ in Eq. (1). The bands are linearized with Fermi velocity $v_F \approx \sqrt{3} t_0$. To study the qualitative properties of the model with parameters relevant for Sr₂RuO₄ it proves useful to express the two spin and the two orbital degrees of freedom through the charge (ϕ_ρ), spin (ϕ_s), flavor (ϕ_f), and spin-flavor (ϕ_{sf}) Bose fields and their conjugate momenta (Π_μ). The representation can be simplified by rotating the reference frame through $\bar{x} = \frac{1}{\sqrt{2}}(x + y)$ and $\bar{y} = \frac{1}{\sqrt{2}}(x - y)$ with $\bar{\mathbf{r}} = (\bar{x}, \bar{y})^\dagger$. The charge (magnetic) sector Hamiltonian including forward scattering terms is given by

$$H_{c(m)} = \lim_{L \rightarrow \infty} \frac{1}{2} \int_{-L}^L d^2\bar{\mathbf{r}} \left\{ v_F \left(\Pi_{\rho(s)}^2 + \Pi_{f(sf)}^2 \right) + V_{c(m)} \left[\partial_{\bar{x}} \phi_{\rho(s)} + \partial_{\bar{y}} \phi_{f(sf)} \right]^2 + \bar{V}_{c(m)} \left[\partial_{\bar{y}} \phi_{\rho(s)} + \partial_{\bar{x}} \phi_{f(sf)} \right]^2 \right\}, \quad (19)$$

with

$$V_{c(m)} = v_F + (-)U_0 + [U_1 + (-)U_2], \quad (20)$$

$$\bar{V}_{c(m)} = v_F + (-)U_0 - [U_1 + (-)U_2]. \quad (21)$$

Equation (19) is the Hamiltonian of a crossed sliding Luttinger liquid.^{67,68}

In the limit $\bar{V}_m \ll V_m$ the magnetic correlations exhibit dominant one-dimensional contributions along the diagonals of the RuO₂ planes.³² On a mean-field level

the spin ($\mu = s, \bar{\nu} = \bar{y}$) and spin-flavor ($\mu = sf, \bar{\nu} = \bar{x}$) channels decouple.

$$H_\mu = \frac{v_\mu L}{2} \int d\bar{\nu} \left[K_\mu \Pi_\mu^2 + K_\mu^{-1} (\partial_{\bar{\nu}} \phi_\mu)^2 \right]. \quad (22)$$

It is then possible to approximate $H_m \approx H_s + H_{sf}$. The Luttinger liquid parameter K_μ and the velocity v_μ are effective parameters of the theory. In the case of SU(2) symmetry in the spin subspace the interaction term Eq. (23) yields a rescaled $K_\mu \rightarrow K_\mu^* = 1$.

It must be emphasized that the one-dimensional idealization of the magnetic subsystem albeit practical has to be used with caution. As discussed in detail in Ref. 32 in the Fermi liquid regime for $T < 25 \text{ K} \sim \bar{V}_m$ the magnetic correlations are two-dimensional but with corrections imposed by the closeness to one-dimensionality. Here the one-dimensional expressions will be applied to make use of results from the literature available for those systems but a discussion of the expected applicability to the realistic case including the two-dimensional coupling is given at the same time (Secs. III D and III E 1).

The back and umklapp scattering term in the bosonized Hamiltonian is

$$H_{\text{int}} = \frac{U_0}{(2\pi a)^2} \int d^2\bar{\mathbf{r}} \cos \sqrt{4\pi} \phi_s(\bar{\mathbf{r}}) \cos \sqrt{4\pi} \phi_{sf}(\bar{\mathbf{r}}) + \frac{1}{(2\pi a)^2} \int d^2\bar{\mathbf{r}} \cos \left[\sqrt{4\pi} \phi_f(\bar{\mathbf{r}}) - 2\sqrt{2} k_F \bar{y} \right] \times \left(U_1 \cos \sqrt{4\pi} \phi_s(\bar{\mathbf{r}}) + U_2 \cos \sqrt{4\pi} \phi_{sf}(\bar{\mathbf{r}}) \right) + \frac{1}{(2\pi a)^2} \int d^2\bar{\mathbf{r}} \cos \left[\sqrt{4\pi} \phi_\rho(\bar{\mathbf{r}}) - 2\sqrt{2} k_F \bar{x} \right] \times \left(U_2 \cos \sqrt{4\pi} \phi_s(\bar{\mathbf{r}}) + U_1 \cos \sqrt{4\pi} \phi_{sf}(\bar{\mathbf{r}}) \right). \quad (23)$$

The limit $a \rightarrow 0$ and $L \rightarrow \infty$ is understood. Note that the symmetry of the superconducting saddle point (Sec. III B) deduced from the interaction term Eq. (23) is manifestly independent of corrections to the bosonized approach since the energy scale is at least an order of magnitude larger than the correction terms, i.e., $U_{0,1,2} \gg t_{i,h,\perp,z} > \bar{V}_m$ (c.f. Ref. 32).

Equations (19) through (23) are explicitly invariant under the symmetry operations of the tetragonal lattice.

A. Bosonized pair operators

At $\mathbf{q} = 0$ the pair operators defined in Eqs. (6) – (8) are local, i.e., $P_{a,b}(\mathbf{q} = 0) = \sum_{\mathbf{l}} P_{a,b}(\mathbf{l})$. The correlations in the $P_{0,\pm}$ channel have been shown to be negligible with respect to the mixed flavor channels in Sec. II A. In the continuum representation the pair operators can be given in terms of the Bose fields as introduced in Ref. 32. The abbreviations $\cos \sqrt{\pi} \phi_\mu(\bar{\mathbf{r}}) = c\phi_\mu$, $\sin \sqrt{\pi} \phi_\mu(\bar{\mathbf{r}}) = s\phi_\mu$, $\cos \sqrt{\pi} \theta_\mu(\bar{\mathbf{r}}) = c\theta_\mu$, $\sin \sqrt{\pi} \theta_\mu(\bar{\mathbf{r}}) = s\theta_\mu$, as well as $\bar{\phi}_f =$

$\phi_f - \sqrt{2/\pi} k_F \bar{y}$ and $\bar{\phi}_\rho = \phi_\rho - \sqrt{2/\pi} k_F \bar{x}$ are introduced for clarity. The pair operator components Eqs. (7) and (8) then are

$$P_{1,+}(\bar{\mathbf{r}}) \propto \frac{2e^{-i\sqrt{\pi}\theta_\rho}}{\pi a} \left[c\theta_{sf} c\bar{\phi}_f c\phi_s + i s\theta_{sf} s\bar{\phi}_f s\phi_s \right. \\ \left. + c\theta_{sf} c\bar{\phi}_\rho c\phi_{sf} + i s\theta_{sf} s\bar{\phi}_\rho s\phi_{sf} \right] \quad (24)$$

$$P_{1,-}(\bar{\mathbf{r}}) \propto \frac{-2e^{-i\sqrt{\pi}\theta_\rho}}{\pi a} \left[c\theta_{sf} s\bar{\phi}_f s\phi_s + i s\theta_{sf} c\bar{\phi}_f c\phi_s \right. \\ \left. + c\theta_{sf} s\bar{\phi}_\rho s\phi_{sf} + i s\theta_{sf} c\bar{\phi}_\rho c\phi_{sf} \right] \quad (25)$$

$$P_{2,+}(\bar{\mathbf{r}}) \propto \frac{2e^{-i\sqrt{\pi}\theta_\rho}}{\pi a} \left[c\theta_s c\bar{\phi}_f c\phi_{sf} + i s\theta_s s\bar{\phi}_f s\phi_{sf} \right. \\ \left. + c\theta_s c\bar{\phi}_\rho c\phi_s + i s\theta_s s\bar{\phi}_\rho s\phi_s \right] \quad (26)$$

$$P_{2,-}(\bar{\mathbf{r}}) \propto \frac{-2e^{-i\sqrt{\pi}\theta_\rho}}{\pi a} \left[c\theta_s s\bar{\phi}_f s\phi_{sf} + i s\theta_s c\bar{\phi}_f c\phi_{sf} \right. \\ \left. + c\theta_s s\bar{\phi}_\rho s\phi_s + i s\theta_s c\bar{\phi}_\rho c\phi_s \right] \quad (27)$$

The limit $a \rightarrow 0$ is understood. The Klein factors have not been plotted here for lucidity but are of crucial importance in the present model of multiple electron species when calculating correlation functions. They do not intervene with the symmetry arguments for the static expectation values discussed below.

A similar analysis of the spin density operators

$$S^\mu(\mathbf{l}) = \sum_{\sigma,\sigma'} \sum_{\nu=x,y} \sigma_{\sigma,\sigma'}^\mu c_{l,\nu,\sigma}^\dagger c_{l,\nu,\sigma'} \quad (28)$$

reveals that the out-of-plane component $S^z(\mathbf{l}) \sim f(\phi_s, \phi_{sf})$ depends on the Bose fields while the in-plane components $S^x(\mathbf{l}) \sim S^y(\mathbf{l}) \sim f(\theta_s, \theta_{sf})$ depend on the dual fields. The $\sigma_{\sigma,\sigma'}^\mu$ are the Pauli matrices. Consequently $K_s^* < K_{sf}^* \leq 1$ is consistent both with the observed magnetic easy plane configuration in Sr_2RuO_4 (Sec. IV A and Ref. 41) and with $\chi_{1,b}^{(P)}(\mathbf{q}, \omega) < \chi_{2,b}^{(P)}(\mathbf{q}, \omega)$. $\chi_{a,b}^{(P)}$ was defined in Eq. (11). The bosonized model is consistent with the superconducting phase transition in the $\{P_{2,+}, P_{2,-}\}$ sector.

As discussed in Sec. II C of Ref. 32 the bosonized approach neglects the exchange terms of Hund's rule coupling. This leads to an underestimation of the $S^z = 0$ spin-triplet component $P_{1,+}$. The μSR measurements¹⁶ discussed in Sec. IV A and the upper critical fields (Ref. 41) suggest that $\langle P_{1,+} \rangle \approx 0.8 \langle P_{2,+} \rangle \approx 0.8 \langle P_{2,-} \rangle$. Since this is close to the isotropic limit $\chi_{1,+}^{(P)}(\mathbf{q}, \omega) \approx \chi_{2,\pm}^{(P)}(\mathbf{q}, \omega)$ will be assumed while $\chi_{1,-}^{(P)}(\mathbf{q}, \omega) < \chi_{1,+}^{(P)}(\mathbf{q}, \omega)$ and consequently the spin-singlet component does not contribute, i.e., $\langle P_{1,-} \rangle = 0$. The instability occurs in the spin-triplet channel consistent with the results in Sec. II A.

B. Order parameter

From Eqs. (24), (26) and (27) follows that the finite value of the order parameter $\langle P_{2,\pm} \rangle, \langle P_{1,+} \rangle \neq 0$ implies $\langle \exp(-i\sqrt{\pi}\theta_\rho) \rangle \neq 0$. This is incompatible⁶⁶ with finite expectation values of operators containing the dual field and thus terms $\sim \cos \sqrt{\pi} \bar{\phi}_\rho$ and $\sim \sin \sqrt{\pi} \bar{\phi}_\rho$ are discarded.

The interaction that led to the derivation of H_{mf} in Eq. (16) is attractive. A Tomonaga-Luttinger model with attractive interaction scales to strong coupling under a renormalization group analysis and has a gapped excitation spectrum.^{64,42} Its thermodynamic properties can be modeled via the sine-Gordon model.⁶⁹⁻⁷² The free energy is lowered proportional to the square of the excitation gap.^{73,63} The energy can be minimized by maximizing the gap. This suggests the minimization of the repulsive components of the interaction term H_{int} through $\langle \cos \sqrt{4\pi} \phi_s \rangle = \langle \cos \sqrt{4\pi} \phi_{sf} \rangle = \langle \cos \sqrt{4\pi} \bar{\phi}_f \rangle = \langle \cos \sqrt{4\pi} \bar{\phi}_\rho \rangle = 0$. It is then consistent to assume that these operators are irrelevant and consequently the contributions $\sim \cos \sqrt{\pi} \phi_s, \sim \cos \sqrt{\pi} \phi_{sf}, \sim \cos \sqrt{\pi} \bar{\phi}_f,$ and $\sim \cos \sqrt{\pi} \bar{\phi}_\rho$ in the operators $P_{2,\pm}$ and $P_{1,+}$ can be neglected.

One then obtains a gap in all channels $\mu \in \{c, s, sf\}$ ⁷⁴ with possible finite expectation values for $\langle \sin \sqrt{\pi} \phi_{sf} \rangle, \langle \sin \sqrt{\pi} \theta_s \rangle, \langle \cos \sqrt{\pi} \theta_s \rangle,$ and $\langle \sin \sqrt{\pi} \bar{\phi}_f \rangle$ as will now be discussed in detail.

The system is invariant under a global phase shift in the charge sector. The fluctuations of the charge phase are referred to as the Anderson-Goldstone collective mode.⁷⁵ They can be parameterized by introducing the unit vector

$$\boldsymbol{\Omega}_\rho = \begin{pmatrix} -i \sin \sqrt{\pi} \theta_\rho \\ \cos \sqrt{\pi} \theta_\rho \end{pmatrix}. \quad (29)$$

The Anderson-Goldstone collective mode results from a broken Gauge symmetry and in the presence of long range Coulomb interaction acquires a gap of the order of the plasma frequency through the Anderson-Higgs mechanism.^{75,43} The large gap allows for neglecting the charge phase fluctuations in the discussions of the low energy excitations that follow (Sec. III E).

Correspondingly, fluctuations of $P_{2,+}$ and $P_{2,-}$ can be parameterized as phase fluctuations in the spin channel via θ_s which takes the role of a azimuthal angle of the magnetic moment of the Cooper pairs. The third spin-triplet component $P_{1,+}$ can be included via a polar angle θ_z .

$$\boldsymbol{\Omega}_s = \begin{pmatrix} -i \sin \sqrt{\pi} \theta_s \sin \theta_z \\ \cos \sqrt{\pi} \theta_s \sin \theta_z \\ \cos \theta_z \end{pmatrix} \quad (30)$$

The $\text{SO}(3)$ vector $\boldsymbol{\Omega}_s$ describes the three spin-triplet components introduced in Sec. II A.

The order parameter expectation values $\langle P_{2,\pm} \rangle, \langle P_{1,+} \rangle \sim \langle \sin \sqrt{\pi} \phi_f \rangle = \langle \sin(\sqrt{\pi} \phi_f - \sqrt{2} \bar{y}) \rangle$ break the invariance of the model under reflection $y \rightarrow -y$. This is an artifact of the mean-field decoupling Eq. (15) which yields only one of two equivalent saddle points. In the absence of external fields, temperature gradients, or strain the symmetry must be restored by including another two-component vector^{76,77}

$$\mathbf{\Omega}_f = \begin{pmatrix} \sin(\sqrt{\pi} \phi_f - \sqrt{2} \bar{y}) \\ \sin(\sqrt{\pi} \phi_f - \sqrt{2} \bar{x}) \end{pmatrix}. \quad (31)$$

Equation (31) includes a p -wave component of the pair operator. This becomes apparent in the rewritten form

$$\mathbf{\Omega}_f = \begin{pmatrix} \cos \sqrt{2} \bar{y} \sin \sqrt{\pi} \phi_f \\ \cos \sqrt{2} \bar{x} \sin \sqrt{\pi} \phi_f \end{pmatrix} - \begin{pmatrix} \sin \sqrt{2} \bar{y} \cos \sqrt{\pi} \phi_f \\ \sin \sqrt{2} \bar{x} \cos \sqrt{\pi} \phi_f \end{pmatrix}. \quad (32)$$

Since the component $\Omega_{f,x}$ is oscillatory along \bar{y} the pair correlations are stronger along \bar{x} and vice versa. The existence of such two order parameter components that couple differently to magnetic fields through a slight spatial anisotropy has been implied experimentally via upper critical field^{23,77,41} and thermal conductivity²¹ measurements as discussed closer in Sec. IV E. The fluctuations of $\mathbf{\Omega}_f$ account for the observed strain anomalies⁴⁹ in the superconducting phase (Sec. III E).

Introducing the normalized average

$$\bar{\mathbf{\Omega}}_\mu = \langle \mathbf{\Omega}_\mu \rangle / |\langle \mathbf{\Omega}_\mu \rangle| \quad (33)$$

$|\bar{\mathbf{\Omega}}_\mu|^2 = 1$ is satisfied. Denoting the order parameter amplitude

$$\bar{P} = |\langle P \rangle| = \frac{2}{\pi} |\langle \sin \sqrt{\pi} \phi_{sf} \rangle| |\langle \mathbf{\Omega}_\rho \rangle| |\langle \mathbf{\Omega}_s \rangle| |\langle \mathbf{\Omega}_f \rangle| \quad (34)$$

the mean-field Hamiltonian Eq. (16) becomes in its continuum representation

$$H_{\text{mf}} = V_0 \int_{-L}^L \frac{d^2 \bar{r}}{a^2} \left[-\bar{P}^2 + \frac{4\bar{P}}{\pi} \sin \sqrt{\pi} \phi_{sf} \left(\bar{\mathbf{\Omega}}_\rho^* \mathbf{\Omega}_\rho \right) \left(\bar{\mathbf{\Omega}}_s^* \mathbf{\Omega}_s \right) \left(\bar{\mathbf{\Omega}}_f^* \mathbf{\Omega}_f \right) \right]. \quad (35)$$

Together with the in-plane contributions Eqs. (19) and (22) the Hamiltonian in the superconducting phase is given by

$$H_{\text{sc}} = H_c + H_s + H_{\text{sf}} + H_{\text{mf}}. \quad (36)$$

C. Magnetic and temperature fields

Magnetic fields need to be included in the microscopic model by introducing a vector potential in the momentum operator.⁷⁸ A detailed study within the model proposed here is rather involved and is left for future studies. One can use the notion of spin-charge separation

thought to discuss some qualitative implications of an applied magnetic field. The coupling of an applied magnetic field \mathbf{h} to the magnetic degrees of freedom of the order parameter then is simply given by

$$H_h = - \int_{-L}^L d^2 \bar{r} \mathbf{h} \bar{\mathbf{\Omega}}_s \quad (37)$$

This term further reduces the symmetry in the spin channel, e.g., $\bar{\mathbf{\Omega}}_s = (\sqrt{2}^{-1}, \sqrt{2}^{-1}, 0)^\dagger$ if the quantization axis is chosen along the applied field. The ground state order parameter then carries spin one along the direction of the magnetic field.

The study of the coupling of an external magnetic field to the anisotropic components of the flavor vector $\mathbf{\Omega}_f$ is more involved. Related two-component superconductors have been studied via a Landau Ginzburg analysis^{76,77} albeit based on p -wave symmetries without the notion of gapless fluctuations addressed in Sec. III E. The general physical result though is that the magnetic field couples strongest to the order parameter component with dominant superconducting correlations perpendicular to the field. If the applied field has a component in the x - y plane, the coupling to the components of $\mathbf{\Omega}_f$ will be inequivalent. A field along \bar{x} will couple stronger to the order parameter component $\Omega_{f,y}$ since it has dominant pair correlations along \bar{y} .

The application of a temperature gradient in the x - y plane breaks the reflection symmetry of the lattice and yields inequivalent components of $\bar{\mathbf{\Omega}}_f$. The order parameter symmetry is reduced to a two-fold axis²¹ perpendicular to the x - y plane as opposed to a four-fold axis in the absence of the temperature gradient. Similar effects are expected through strain⁴⁹ and at surfaces or grain⁷⁹ boundaries.

D. Mapping onto sine-Gordon models

The mean-field contribution Eq. (35) couples all the channels $\mu \in \{\rho, s, f, sf\}$. Since the lowest bound state and thus the gap energy is correctly reproduced by a perturbative treatment even in one-dimensional interacting systems⁶³ one can attempt a mean-field like decoupling valid at least for small values of the fields ϕ_μ . To this end all terms $\sim \sin \sqrt{\pi} \phi_\mu$ and $\sim \sin \sqrt{\pi} \theta_\mu$ are transformed to cos terms via the sliding transformations $\phi_\mu \rightarrow \phi_\mu - \frac{\pi}{4}$ and $\theta_\mu \rightarrow \theta_\mu - \frac{\pi}{4}$. Expanding the cos terms to second order in the fields decouples $H_{\text{mf,eff}}$ in the different channels μ . Rewriting the resulting contributions $H_{\text{mf},\mu}$ in terms of cos and reversing the sliding transformations $\theta_\mu \rightarrow \theta_\mu + \frac{\pi}{4}$ where necessary yields the desired result (up to a constant).

In order to obtain the Lagrangian for the Hamiltonians in Eq. (22) Euclidean time dependence of the fields is introduced, the Lagrange transformation $\Pi_\mu(\bar{\mathbf{r}}, \tau) = \frac{i}{K_\mu^*} \dot{\phi}_\mu(\bar{\mathbf{r}}, \tau)$ is performed, and the fields are rescaled as

$\varphi_\mu = (K_\mu^*)^{-1/2} \phi_\mu$. The effective, one-dimensional action for the spin-flavor channel is obtained as

$$S_{\text{sf}}^{\text{eff}} = \frac{v_{\text{sf}} L}{2} \int_{-L}^L d\bar{y} \int_0^\beta d\tau \left[\dot{\varphi}_{\text{sf}}^2 + (\partial_{\bar{y}} \varphi_{\text{sf}})^2 + \bar{P} M_{\text{sf}} \cos B_{\text{sf}} \varphi_{\text{sf}} \right] \quad (38)$$

with $B_{\text{sf}} = \sqrt{\pi K_{\text{sf}}^*}$ and inverse temperature $\beta = T^{-1}$. Equation (38) is the quantum sine-Gordon action with the interaction parameter $M_\mu = \frac{8V_0}{v_\mu \pi a^2}$.

The transformation to the dual fields $\Pi_\mu = -\partial_{\bar{x}} \theta_\mu$ and rescaling as $\vartheta_\mu = (K_\mu^*)^{1/2} \theta_\mu$ yields the effective, one-dimensional spin-channel action

$$S_s^{\text{eff}} = \frac{v_s L}{2} \int_{-L}^L d\bar{x} \int_0^\beta d\tau \left[\dot{\vartheta}_s^2 + (\partial_{\bar{x}} \vartheta_s)^2 + \bar{P} M_s \bar{\Omega}'_s \Omega'_s \right] \quad (39)$$

for correspondingly adapted vectors $\bar{\Omega}'_s$ and Ω'_s . The action in Eq. (39) is invariant under a rotation of $\bar{\Omega}'_s$. Transversal fluctuations of Ω'_s with respect to $\bar{\Omega}'_s$ give rise to Goldstone modes which can be treated separately as will be done in Sec. III E and Appendix A. To study thermodynamic properties as implied by the sine-Gordon action one can consequently use the simplified expression with $\bar{\Omega}'_s \Omega'_s \rightarrow \cos B_s \vartheta_s$ with $B_s = \sqrt{\pi}/\sqrt{K_s^*}$.⁸⁰

For $T \rightarrow 0$ and $L \rightarrow \infty$ the sine-Gordon actions Eqs. (38) and (39) are equivalent to the charge zero-sector of the massive Thirring model if $B_\mu < 8\pi$.^{81,63} For both channels to be in the gapped regime requires $K_{\text{sf}}^* < 8$ and $K_s^* > 1/8$. Unless $K_s^* < 1$ is very strongly renormalized the conditions on K_μ^* are satisfied.

For $T \rightarrow 0$ and $L \rightarrow \infty$ the actions Eqs. (38) and (39) have a gap of⁶³

$$\Delta_\mu \sim \left[\bar{P} a^2 M_\mu \right]^{\frac{1}{2 - (B_\mu^2)/(4\pi)}} \quad (40)$$

to the lowest bound state above the ground state.

Similarly the action for the charge channel can be derived.

$$S_c = \frac{1}{2} \int_{-L}^L d^2 \bar{r} \int_0^\beta d\tau \left\{ v_{\text{F}} \left(\dot{\phi}_\rho^2 + \dot{\phi}_f^2 \right) + V_c \left[\partial_{\bar{x}} \phi_\rho + \partial_{\bar{y}} \phi_f \right]^2 + \bar{V}_c \left[\partial_{\bar{y}} \phi_\rho + \partial_{\bar{x}} \phi_f \right]^2 + \bar{P} \frac{4V_0}{\pi a^2} \left(\bar{\Omega}'_\rho \Omega'_\rho \right) \left(\bar{\Omega}'_f \Omega'_f \right) \right\}, \quad (41)$$

The action Eq. (41) can be transformed to both dual fields θ_ρ and θ_f but a mixed representation in θ_ρ and ϕ_f as desirable is not possible.

No detailed theoretical results are known for the two-dimensional two-component sine-Gordon model defined by Eq. (41). In the gapped phase relevant here the difference between the two-dimensional correlations and the one-dimensional ones are less severe (Sec. III E 1) then

in the absence of a gap. It is thus permissible to use the theoretical results given in the literature for the one-dimensional actions Eqs. (38) and (39) and anticipating corrections from the two-dimensional character of Eq. (41) and the two-dimensional corrections³² to Eqs. (38) and (39).

E. Fluctuations

The description of Goldstone modes in symmetry broken phases via non-linear sigma models is a standard problem in text book literature.^{82,71,72} The description of the charge phase fluctuations including the Anderson-Higgs mechanism leading to the charge-phase gap has been derived by Schulz⁴³ for the case of the attractive two-dimensional Hubbard model. Goldstone modes of the magnetically ordered phase of the repulsive two-dimensional Hubbard model have been discussed by Schulz^{43,83} and Weng⁸⁴ *et al.* Most importantly, the present approach is a two-dimensional analog of superfluid ³He-A.^{54,55} The conclusive result is that for temperatures sufficiently smaller than the electronic excitation gap $T \ll \Delta$ and at sufficiently small energies $\omega \ll \Delta$ the gapless fluctuations of the internal degrees of freedom of the order parameter associated with continuously broken symmetries are well described by non-linear sigma models (Appendix A).

In the present approach the gapless Goldstone modes correspond to the broken local spin rotational invariance described by the SO(3) vector Ω_s and the degenerate flavor saddle points described by the SO(2) vector Ω_f with local constraints $|\Omega_\mu(\mathbf{r}, \tau)|^2 = 1$.

At sufficiently small temperatures and energy scales $T, \omega \ll \Delta$ the stiffness of the non-linear sigma model describing the angular fluctuations has been determined^{71,72} to scale with the square of the order parameter amplitude $\sim \bar{P}^2$. The analogy to magnetic excitations in the ordered Hubbard model suggest corrections^{84,43} that depend on the specific correlations of the system. The resulting non-linear sigma model in Euclidean space (Appendix A) is⁴³

$$S_\Omega = \bar{P}^2 \int_{-L}^L d^2 r \int_0^\beta d\tau \sum_{\nu, \mu} A_\nu \left[\frac{(\dot{\bar{\Omega}}_\mu)^2}{(av_\nu)^2} + (\partial_\nu \bar{\Omega}_\mu)^2 \right], \quad (42)$$

the stiffness parameters are

$$A_\nu = \frac{\partial^2}{\partial q_\nu^2} \left(V_q^2 \chi_{2, \pm}^{(P)}(\mathbf{q}, 0) \right) \Big|_{\mathbf{q}=0} \quad (43)$$

with the excitation velocities

$$\frac{1}{(v_\nu)^2} = \frac{V_0^2}{A_\nu} \frac{\partial^2}{\partial \omega^2} \chi_{2, \pm}^{(P)}(0, \omega) \Big|_{\omega=0}. \quad (44)$$

Here the magnetic channel is treated isotropically. The pair correlation functions depend on $q_{\bar{x}}, q_{\bar{y}} \sim q_x \pm q_y$.

Consequently $A_x = A_y$ reflecting the symmetry of the lattice. The stiffness perpendicular to the xy plane is negligible since the out-of-plane correlations are two orders of magnitude smaller as indicated by the resistivity,⁷ thermal conductivity,²⁰ and critical magnetic field⁸⁵ measurements. Within the mean-field approach $A_z \equiv 0$. Note that Eqs. (42) through (44) can also be obtained by replacing $X^2 \rightarrow \bar{P}^2$ in the amplitude fluctuation expression Eq. (89) in Appendix B.

The crucial difference of the present model with respect to BCS theory is the presence of gapless modes in the ordered phase. Unlike in BCS the excitations of the internal degrees of freedom of the order parameter, namely the SO(3) spin-triplet components and the SO(2) flavor components do not necessarily acquire a gap (Appendix B2). The analysis of a related model⁸⁶ and the analogy^{54,55} to ³He-A suggests that the magnetic excitations remain gapless and have linear dispersions.⁸⁷ Similar arguments^{54,55} hold for the flavor degrees of freedom.⁸⁸

Note that even in the case of a large gap $\Omega_A \geq \Delta$ of the magnetic fluctuations Ω_s which could in principle induced by the spin-flavor coupling terms in Eq. (23) the physical implications of the present approach remain unaltered because of the ungapped SO(2) flavor mode⁵⁵ Ω_f . The degeneracy of the components of Ω_f are prerequisite for the presence of a gapless flavor mode. At this point it should be stressed that the tetragonal structure of Sr₂RuO₄ has been found to be very stable (c.f. Ref. 2). Since $\Omega_{f,x}$ and $\Omega_{f,y}$ are related via a symmetry operation under which the tetragonal point group of the lattice is invariant it can be concluded that the degeneracy of the two components is also very stable, at least in the bulk material. For a discussion see Sec. (V).

Experimental evidence of the existence of the flavor mode stems from ultrasonic measurements in Ref. 49 that probe the strain dependence of the superconductivity in Sr₂RuO₄. The in-plane anisotropy of the components $\Omega_{f,x}$ and $\Omega_{f,y}$ leads to a coupling of the superconducting order parameter to the strain and thus accounts for the observed effects. The coupling to out-of-plane shear strain components is much weaker. The gapless excitations yield a reduction of the elastic constants in the superconducting phase. The strain breaks the symmetry between the two components which accounts for the anomalies observed near the phase transition. Also, the observed anomalous absorption in cyclotron resonance experiments⁸⁹ might be attributed to the coupling to the Ω_f gapless mode.

1. Estimates for the pair correlation function

On the mean-field level one expects that the pair correlation functions that determine the the stiffness and excitation velocities through Eqs. (43) and (44) have the

form^{90,78}

$$\chi_{\text{BCS}}^{(P)}(\mathbf{q}, \omega) = \frac{-\Delta f(\mathbf{q})}{\omega^2 - \bar{v}_{\text{eff}}^2 \mathbf{q}^2 - \Delta^2}, \quad (45)$$

where Δ is the single particle energy gap, \bar{v}_{eff} is the effective velocity of the collective excitations associated with the pair operators, and $f(\mathbf{q})$ is a function that weakly depends on \mathbf{q} . Note that in the static limit and with a pair correlation length ξ_P related to the superconducting gap⁹⁰ as $\xi_P \propto \bar{v}_{\text{eff}}/\Delta$ the pair correlation function has Lorentzian form $\chi^{(P)}(\mathbf{q} \rightarrow 0, \omega = 0) \sim \xi_P^{-1}(|a\mathbf{q}|^2 + \xi_P^{-2})^{-1}$. Equation (45) is thus valid on a rather general basis.

Since one expects that the quasi one-dimensional correlations exhibit the most singular behavior, and since the normal phase magnetic properties of the system are dominated by quasi one-dimensional correlations,³² it is necessary to investigate the possible impact of the one-dimensional subsystem on the stiffness and excitation velocities through Eqs. (43) and (44).

First of all it must be stated that the scale invariance of the magnetic correlations breaks down³⁵ in the Fermi liquid regime for $T < 25$ K indicating that the system turns two-dimensional at low temperatures.³² Furthermore, the pair correlation functions factorize into spin, spin-flavor, charge, and flavor contributions in the bosonized representation [c.f., Eqs. (24) through (27)]. In the superconducting phase the correlation functions have to be evaluated with respect to the actions Eqs. (38), (39), and (41) where all channels are gapped. Consequently in the superconducting phase the divergent correlations of the quasi one-dimensional magnetic subsystem are suppressed and $\chi_{2,\pm}^{(P)}(\mathbf{q}, \omega)$ is analytic in \mathbf{q} and ω . The contributions from the charge and flavor channels are two dimensional anyway [Eq. (41)].

To make these reflections more transparent consider that for $T > T_c$ the spin and spin-flavor channel correlation functions are approximately determined by the Hamiltonian Eq. (22). They have the standard functional dependence in conformal field theory.^{91,71} Density and pair correlation functions are connected via substituting $|2k_F - q_{\mathcal{T}}| \rightarrow q_{\mathcal{T}}$ with Fermi wavenumber k_F and an appropriate adoption of the scaling dimension.⁶⁴ Dimerized spin chains are described by the action Eq. (38) with⁹² $B_\mu^2 = 2\pi$ and the density correlation functions have been given in Ref. 40. The value of $B_\mu^2 = 2\pi$ is not a singular point in the analysis⁶³ at $T = 0$ and similar behavior for other values of B_μ^2 is expected, especially at finite temperatures. This leads to the estimate⁴⁰

$$\chi_{\text{1D}}^{(P)}(q_{\mathcal{T}}, \omega) = \frac{A_0 \cos^2(aq_{\mathcal{T}}/2)}{\omega^2 - \bar{v}_{\text{eff}}^2 \sin^2(aq_{\mathcal{T}}) - \Delta^2}, \quad (46)$$

where Δ is the energy gap to the lowest bound state. Comparing with Eq. (45) one consequently finds that in the gapped phase $\chi_{\text{1D}}^{(P)}(q_{\mathcal{T}}, \omega) \equiv \chi_{\text{BCS}}^{(P)}(q_{\mathcal{T}}, \omega)$ with

$-\Delta f(q_{\overline{\nu}}) = A_0 \cos^2(aq_{\overline{\nu}}/2)$. Moreover, $\chi_{1D}^{(P)}(q_{\overline{\nu}}, 0)$ is analytic in $q_{\overline{\nu}} = 0$. This result is not surprising in the light of the relevant three-dimensional couplings that have to be present in order to drive any quasi one-dimensional system into the ordered phase.⁴⁰

In Appendix B1 it is shown that the analytical properties of the pair correlation functions $\chi_{2,\pm}^{(P)}$ are related to those of $\chi_{\text{BCS}}^{(P)}$ [c.f. Eq. (88)]. Given the analyticity of the one-dimensional contribution Eq. (46), the coupling terms that render the magnetic system two-dimensional below³² $T < 25$ K, and the two-dimensionality of the charge contribution as shown in Eq. (41) it can be concluded that the A_ν as defined in Eq. (43) are dominantly isotropic in the q_x - q_y plane for $T \ll \overline{v}_{\text{eff}}$ and $q_\nu \ll a^{-1}$ up to quadratic order in q_ν .

From the geometry of the upper critical magnetic fields discussed in Ref. 41 it can be concluded that there is an in-plane anisotropy in the order parameter of $\sim 7\%$ which should be reflected also in $\chi_{2,\pm}^{(P)}$. Most importantly, the non-analyticity along the diagonals of the basal plane⁴¹ suggests the presence of a small term $\sim |q_x q_y|$ in the expansion of $\chi_{2,\pm}^{(P)}$. Considering the small energy scale set by the anisotropic component of the upper critical magnetic field $H_{c,a}(T \rightarrow 0) \approx 0.05$ T ~ 0.04 K the effect should be negligible here for $T \geq 0.1$ K. The expected significant next higher order anisotropic correction terms are $\sim q_x^2 q_y^2$.

2. Effective Saddle point

The amplitude fluctuations of the order parameter become relevant on energies scales of the order of the excitation gap $\omega \sim \Delta$ (or, equivalently, for wavevectors $a|q_\nu| \sim \Delta/v_\nu$) and qualitatively change the behavior of the gapless modes at these energy scales (Appendix B). The description of the latter via the non-linear sigma models in Eq. (42) is consequently restricted to small temperatures, small energies, and large wavelengths.⁷¹

As the gap decreases while the system approaches the phase transition thermal fluctuations become sufficiently large to excite the amplitude mode which in turn couples back to the angular Goldstone modes. Amplitude fluctuations at energy scales of the order of or larger than the gap can be treated outside the critical region by the standard approach⁹³ where Gaussian fluctuations are integrated out. In Appendix B2 it is shown that the Gaussian amplitude fluctuations can be included in the description of the $\overline{\Omega}_\mu$ modes in Fourier space in form of a cutoff and a fluctuation dependent prefactor:

$$S_\Omega^{\text{amp}} \approx \frac{\beta N}{4\pi^2} \langle X^2 \rangle \sum_{\nu, \mu, n}^{0 < \omega_n < \Delta} A_\nu \int_0^{\Delta/v_\nu} d^2[aq] \left[\frac{\omega_n^2}{v_\nu^2} + [aq_\nu]^2 \right] \overline{\Omega}_\mu^2. \quad (47)$$

The number of in-plane Ru ions is $N = L^2/a^2$ and the prefactor $\langle X^2 \rangle$ is the variance of the amplitude fluctuations and parameterizes the effect of the amplitude fluctuations on the action of the Goldstone modes. Following the analysis in Appendix B one can approximate $\beta \langle X^2 \rangle \approx \chi_{\text{BCS}}^{(P)}(0, 0) = \frac{f_0}{\Delta}$ [Eq. (83)]. Near the phase transition, where $\Delta \rightarrow 0$, the prefactor diverges which is reminiscent of the diverging correlation length.⁴³ For $T \rightarrow T_c$ one has $S_\Omega^{\text{amp}} \gg S_\Omega$ and the impact of the fluctuations of the internal degrees of freedom of the order parameter is determined by Eq. (47).

A dimensional analysis suggests that the integrals in Eq. (47) are proportional to Δ^5 . Using $A_\nu \approx \frac{\overline{v}_{\text{eff}}^2}{\Delta f_0}$ [Eq. (84)], and $v_\nu \approx \overline{v}_{\text{eff}}$ [Eq. (85)] the contribution to the action from the amplitude-Goldstone mode coupling term can thus be estimated to be

$$S_\Omega^{\text{amp}} \approx \frac{s_0^2 \beta N}{4\pi^3 \overline{v}_{\text{eff}}^2} \Delta^3 + \text{O}(\Delta^5). \quad (48)$$

The approximation is justified when the stiffness $\rho_s^{\text{amp}} \approx \beta \langle X^2 \rangle A_\nu \approx T \frac{\overline{v}_{\text{eff}}^2}{\Delta^2}$ is large enough, i.e., in the limit $\Delta \rightarrow 0$. In this approximation all channels μ yield the same contribution. The dimensionless prefactor $s_0^2 \sim 1$ is phenomenological since the exact numerical prefactor is not known within the approximations made.

Equation (48) is an effective saddle point contribution in which the fluctuations of the internal degrees of freedom of the order parameter have effectively been integrated out. The approach is only applicable outside the critical region $T \leq T_c - 0.02$ K (Appendix B3).

The contribution from Eq. 48 is of third order in the gap Δ^3 near the phase transition. This an important consequence of the two dimensionality of the problem. In one or three dimensions the contribution is Δ^2 or Δ^4 , respectively, and consequently only renormalizes the usual parameters⁹⁴ of a Landau expansion.

F. Free energy

The general expression of the total free energy consists of the contributions from the spin, spin-flavor, and charge channels and the mean-field contribution, i.e., $F = \sum_\mu F_\mu + F_{\text{mf}}$, with

$$F_\mu = -T \ln \int d\varphi_\mu e^{-S_\mu} \quad \text{for } \mu \in \{\text{sf}, \text{c}\}, \quad (49)$$

$$F_\mu = -T \ln \int d\vartheta_\mu e^{-S_\mu} \quad \text{for } \mu \in \{\text{s}\}, \quad (50)$$

where $d\varphi_c = d\phi_\rho d\phi_f$. The actions S_μ are given by Eqs. (38), (39), and (41) with $(P) = 0$ in the normal phase. The mean-field contribution is

$$F_{\text{mf}} = -V_0 N \overline{P}^2 - T \ln \int \left[\prod_{\mathbf{q}, n} \frac{d\overline{\Omega}_f}{(2\pi)} \frac{d\overline{\Omega}_s}{(4\pi)} \right] e^{-S_\Omega}. \quad (51)$$

The second term accounts for the gapless fluctuations of the internal degrees of freedom of the order parameter (Sec. III E and Appendix).

The order parameter is obtained by minimizing the free energy via the variation $(\delta F)/(\delta \bar{P}) = 0$. At finite temperatures the analysis of the expectation values of the sine-Gordon and related models is quite involved.⁹⁵ An estimate of the symmetry of the full Eliashberg equation is discussed phenomenologically in Ref. 34. Based on the result that interaction effects can render the gap function rather homogeneous in agreement with the experimental results⁴¹ (Sec. IV E) one can derive a Landau theory for the free energy near the phase transition in the ordered phase.

To this end we omit at the moment the contribution from the fluctuation action S_Ω , assume an isotropic order parameter,^{34,41} and consider the resulting self-consistency equation which reads

$$\bar{P} = \frac{2}{L^2 V_0} \sum_\mu \frac{\delta F_\mu}{\delta \bar{P}}. \quad (52)$$

To obtain an estimate for Eq. (52) we make use of the equivalence of the actions Eq. (38) and (39) to those of spin chains with alternating interactions.⁴⁰ The self-consistency Eq. (52) is thus equivalent to that studied in the context of the spin-Peierls transition in CuGeO_3 studied in Ref. 96. The results show that a one-dimensional system that undergoes a phase transition to long range order—induced by an effective three-dimensional coupling that can be treated mean-field like—can be described near the phase transition by the standard mean-field free energy functional⁹⁴

$$\left[\sum_\mu F_\mu + F_{\text{mf}} \right]_{T \sim T_c} = \sum_\mu F_{0,\mu} + NV_0 \left[\frac{T}{T_c} - 1 \right] \bar{P}^2 + Nb \bar{P}^4 \quad (53)$$

and consequently

$$\left[\sum_\mu F_\mu \right]_{T \sim T_c} = \sum_\mu F_{0,\mu} + NV_0 \frac{T}{T_c} \bar{P}^2 + Nb \bar{P}^4. \quad (54)$$

By analogy we adapt this description near the phase transition while for $T \rightarrow 0$ the free energy saturates as^{73,63,97}

$$F_\mu(T=0) \sim \bar{P}_0^{-\frac{1}{1-(B_\mu^2)/(8\pi)}}. \quad (55)$$

The dimerized spin chain is $\text{SU}(2)$ invariant with $B_\mu^2 = 2\pi$.^{98–100} Since $B_\mu^2 = 2\pi$ is not a singular point in the analysis⁶³ at $T = 0$ similar behavior for other values of B_μ can be expected at finite temperature. The comparison of Eqs. (54) and (55) yields an effective finite temperature interaction parameter of

$$B_\mu^2(T \sim T_c) \approx 4\pi, \quad (56)$$

which is the value for free massive fermions.⁷² Near T_c Eq. (40) then yields a gap of⁶³

$$\Delta \approx 8 V_0 \bar{P}. \quad (57)$$

As discussed in Sec. III E 2 the the gapless fluctuation contribution at the phase transition can be described via the effective saddle point term Eq. (48), i.e., $S_\Omega \rightarrow S_\Omega^{\text{amp}}$ in Eq. (51). Together with Eq. (53) the Landau expansion of the free energy F_Δ near the phase transition then is

$$\frac{F_\Delta}{N} = \frac{\sum_\mu F_{0,\mu}}{N} - V_0 t \bar{P}^2 + \frac{4V_0^3 s_0^2}{\bar{v}_{\text{eff}}^2} \bar{P}^3 + b \bar{P}^4 + \dots, \quad (58)$$

where $t = 1 - T/T_c \ll 1$ is the reduced temperature. The approach is valid outside the critical region, i.e., for $|t| \geq 0.01$ as estimated in Appendix B3. Since the expansion is in $\bar{P} \geq 0$ and *not* in the complex order parameter the phase transition described by Eq. (58) is of third order in the sense of Ehrenfest's definition.¹⁰¹ Gauge invariance is preserved since $\bar{P} = |e^{i\phi_G} \langle P \rangle|$ for arbitrary gauge fields ϕ_G .

IV. APPLICATION TO Sr_2RuO_4

The inter-plane coupling in Sr_2RuO_4 leads to a superconducting ground state driven by the d_{zx} and d_{yz} correlations. The d_{zx} and d_{yz} correlations are described by the model derived in Ref. 32 and applied in Sec. III. The pair order parameter is the expectation value of orbital-singlet, spin-triplet Cooper pairs. The gapless fluctuations of the multiple order parameter components are dominantly two dimensional. In this section the physical implications of the model are compared with the properties of Sr_2RuO_4 determined through experiments.

A. Order parameter: μSR and excess tunneling current

Minimizing the Landau expansion of the free energy Eq. (58) via $(\partial F_\Delta)/(\partial \bar{P}) = 0$ gives

$$\bar{P}|_{t \ll 1} = \frac{3V_0^3 s_0^2}{2b \bar{v}_{\text{eff}}^2} \left[\sqrt{1 + \frac{32b \bar{v}_{\text{eff}}^4 t}{9V_0^5 s_0^4}} - 1 \right] \approx \frac{\bar{v}_{\text{eff}}^2}{6V_0^2 s_0^2} t. \quad (59)$$

The slope $\frac{\bar{v}_{\text{eff}}^2}{6V_0^2 s_0^2} \approx 0.1$ has been determined from the analysis of the specific heat data in Sec. IV B. For $T \rightarrow 0$ or $t \rightarrow 1$ Nernst's theorem requires the order parameter to saturate. A corresponding fit function to the experimental data as shown in Fig. 1 yields using Eq. (57)

$$\Delta(T) = \left(5 - \sqrt{1 + 11T^2/\text{K}^2} \right) \text{K} \quad (60)$$

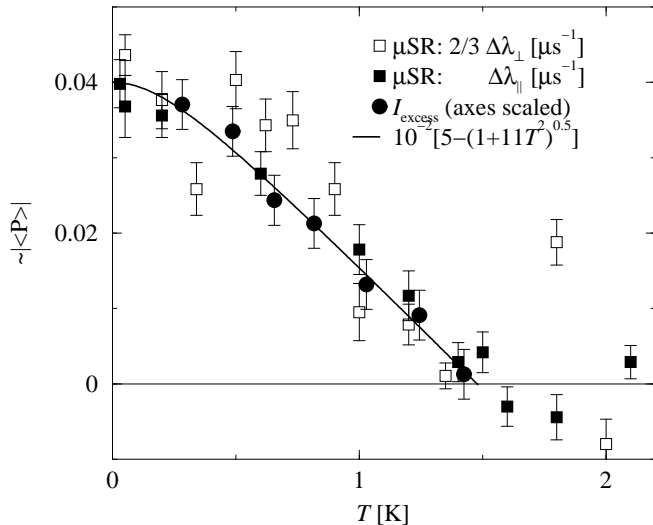


FIG. 1. Order parameter as a function of temperature. Circles are the excess current from Ref. 17 (axes scaled), squares are μSR relaxation rates from Ref. 16 with subtracted normal phase relaxation rate. Full squares are for Muon spins polarized in the x - y plane, open squares are scaled with $2/3$ for Muon spins polarized perpendicular to the x - y plane. The phenomenological fit $10^{-2}(5 - \sqrt{1 + 11T^2})$ [Eq. (60)] is consistent with the linear temperature dependence of the order parameter predicted in Eq. (59).

and is consistent with Eq. (59) for $T_c = 1.48$ K. Note that the determination of T_c from experiments for an order parameter linear in t is slightly different than in the case without gapless fluctuations where $\Delta \sim \sqrt{t}$, see Sec. IV B.

The squares in Fig. 1 show the increase of the μSR relaxation rates $\Delta\lambda_{\perp}$ (open symbols, Muon spin polarized perpendicular to the x - y plane) and $\Delta\lambda_{\parallel}$ (full symbols, Muon spin polarized parallel to the x - y plane) below the superconducting phase transition from Ref. 16. The increase of the μSR relaxation rate is a consequence of the gapless magnetic fluctuations induced by the spin-triplet Cooper pairs in the superconducting phase and described by $\overline{\Omega}_s$. The magnetic excitations can scatter dynamically off the Muon spins. The resulting coupling to the Muon spin must be described in the dynamical limit as¹⁰²

$$\lambda_s = B_0^2 \tau_s^{-1}. \quad (61)$$

B_0 is the field at the Muon site, τ_s^{-1} is the Cooper pair spin scattering rate. From the absence of any change in the static susceptibility^{14,15} can be concluded that B_0 is the same in both the normal phase and the superconducting phase. The absence of the $\overline{\Omega}_s$ fluctuations in the normal phase yield $\lambda_s \gg \lambda_n$, where λ_n is the Muon relaxation rate induced by the “normal” electrons. Since the contribution from the Cooper pairs is $\sim \lambda_s \overline{P}/\overline{P}_0$ while that from the “normal” electrons is $\sim \lambda_n(1 - \overline{P}/\overline{P}_0)$ one has

$$\Delta\lambda = (\lambda_s - \lambda_n) \overline{P}/\overline{P}_0. \quad (62)$$

The results from μSR are consistent with the linear temperature dependence of the order parameter (Fig. 1).

In the presence of an external magnetic field the magnetic components of the order parameter are Zeeman split as discussed in Sec. III C. The spin scattering rate τ_s^{-1} and thus λ_s are exponentially suppressed. This is consistent with the experimental observation.¹⁶

As mentioned in Sec. III E the spin-flavor coupling terms in Eq. (23) could in principle lead to a gap in the magnetic excitation spectrum. On the other hand such a coupling would inevitably add a magnetic component to the flavor degrees of freedom. Since the $\text{SO}(2)$ flavor fluctuations remain gapless⁵⁵ the Muon spin would then couple dynamically to the magnetic moment of the flavor mode leaving the physical picture of the origin of the increase of the μSR relaxation rate unaltered.

From $\Delta\lambda_{\parallel} \approx 2/3\Delta\lambda_{\perp}$ it can be concluded that the spin-one Cooper pairs are in a slight easy plane configuration, i.e., $B_{\perp} \approx 0.8B_{\parallel}$. Note that $\Delta\lambda_{\parallel} \sim B_{\perp}^2$ and vice versa.¹⁰² From the critical field analysis in Ref. 41 the in-plane moment can be determined more precisely to be enhanced by a factor 1.23 with respect to the out-of-plane moment.

The excess current across a normal-superconducting point contact is proportional to the superconducting gap at least in s -wave superconductors.¹⁰³ As discussed in Sec. II C and Ref. 34 the order parameter in Sr_2RuO_4 has extended s -wave character and in Sec. IV E the superconducting gap in Sr_2RuO_4 is determined to be 93% isotropic. The full circles in Fig. 1 are excess current data from Ref. 17 and are in striking agreement with the linear temperature dependence of the order parameter. The data are scaled to match T_c and the slope.

Equation (60) gives an energy gap of $\Delta|_{T \rightarrow 0} \approx 0.33$ meV. The results from the differential resistance versus bias voltage measurements across point contact junctions depend on the model used for their analysis. A p -wave analysis without gapless excitations yields $\Delta|_{T \rightarrow 0} \approx 1.1$ meV, a s -wave analysis $\Delta|_{T \rightarrow 0} \approx 0.25$ meV.¹⁷ Both results are close to the value extracted here.

The differential resistance data have been argued to be inconsistent with an isotropic s -wave superconductor in the absence of gapless excitations.^{17,18} The theoretical approach in Ref. 104 supports this conclusion but ignores contributions from the d_{zx} and d_{yz} orbitals. An analysis of the Andreev reflection spectroscopy data in the presence of the herein discussed order parameter including massless fluctuations is desirable.

Within the p -wave approach proposed in the literature^{11,53} the order parameter $\mathbf{d}(\mathbf{k}) = \hat{z}(k_x \pm ik_y)$ breaks time reversal symmetry and thus can also explain the change in the Muon relaxation rate^{16,6} at the superconducting phase transition. The resulting temperature dependence of the order parameter enters via the local field and is consequently $\sim \sqrt{t}$ consistent with the differential resistance analysis¹⁷ but not with the measured linear temperature dependence of the excess current. On

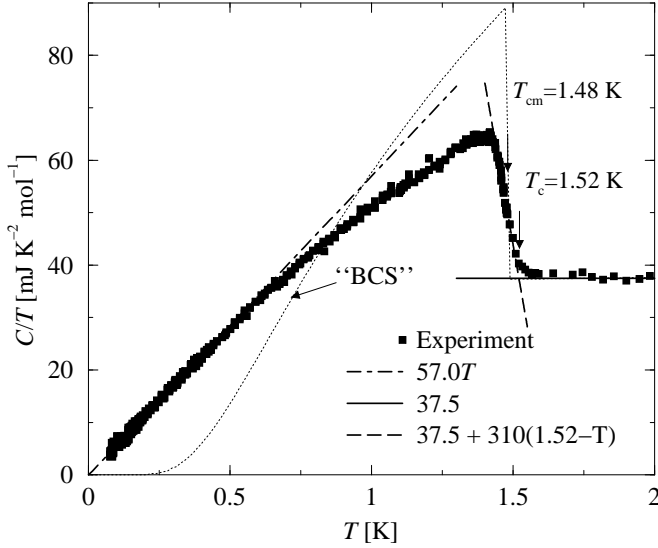


FIG. 2. Specific heat over temperature as a function of temperature. Symbols are from Ref. 30. $T_{\text{cm}} = 1.48$ K is the “mid transition” value. The actual transition is at $T_c = 1.52$ K. In the normal phase the specific heat is linear (full line) consistent with Fermi or Luttinger liquid behavior.³² For T just below T_c a linear increase with $t = 1 - T/T_c$ is observed consistent with an order parameter linear in t [Eq. (63)]. For $T < 0.3$ K the specific heat is quadratic in temperature [dot-dashed line, Eq. (64)] consistent with two-dimensional, gapless order parameter fluctuations. Dotted line: sketch of the BCS contribution.

the other hand, the excess current might be dominated by surface effects not considered here. A more obvious possible shortfall of the p -wave approach are the neutron scattering results³⁵ that do not show any signature of a gap down to energy transfers of $\omega \geq 1$ meV suggesting that $2\Delta < 1$ meV which is inconsistent with the gap value¹⁷ of $\Delta|_{T \rightarrow 0} \approx 1.1$ meV discussed above.

B. Specific heat

The normal phase thermodynamic properties have been described satisfactorily in the framework of the model outlined in Ref. 32. The specific heat $C_n^{\text{tot}} \approx 37.5 \frac{\text{mJ}}{\text{K}^2 \text{mol}} T$ is linear in temperature for $T_c < T < 30$ K as is shown by the solid line in Fig. 2.

In the superconducting phase near the phase transition, i.e., $t = 1 - T/T_c \ll 1$, the free energy is given by F_Δ in Eq. (58) while the temperature dependence of the superconducting pair density \bar{P} is given by Eq. (59). The resulting specific heat $C_s = -T \partial^2 F_\Delta / (\partial T^2)|_{t>0}$ is

$$\frac{C_s|_{t \ll 1}}{T_c} = \frac{C_n^{\text{tot}}}{T_c} + 2 \left[\frac{\bar{v}_{\text{eff}}^2}{6 V_0^2 s_0^2} \right]^2 \frac{V_0}{T_c^2} t - O(t^2). \quad (63)$$

For $V_0 = 6$ K (see Sec. II A) and $T_c = 1.52$ K according to the fit in Fig. 2 (dashed line) one has $\frac{\bar{v}_{\text{eff}}^2}{6 V_0^2 s_0^2} \approx 0.1$ which

is consistent with the measured superconducting energy gap as discussed in Sec. IV A. One finds $\bar{v}_{\text{eff}}^2/s_0^2 \approx 22 \text{ K}^2$. Note that the “mid transition” temperature $T_{\text{cm}} = 1.48$ K is slightly lower than the critical temperature $T_c = 1.52$ K determined here.

For slightly lower temperatures, i.e., $t > 0.05$, the negative, higher order terms in Eq. (63) quickly become dominant. For temperatures $0.7 > t > 0.05$ the experimental specific heat is given by a superposition of the exponential term from the gapped electronic charge, spin, and spin flavor channels F_μ [Eqs. (49) and (50)] and from the non-linear sigma model [Eq. (47)].

The appropriate sine-Gordon actions for the electronic channels are given by Eqs. (38), (39), and (41). With finite $M_\mu \neq 0$ they yield a BCS-like, exponential specific heat contribution as sketched by the dotted line in Figure 2. The fluctuation contribution from the non-linear sigma model Eq. (47) to the specific heat in Eq. (63) is negative $\sim -t$ for $t \rightarrow 0$. Consequently the gapless fluctuations account for the jump in the specific heat at T_c that is lower than anticipated by a gapped mean-field calculation.³⁰ The physical interpretation is that a significant contribution to the entropy is contained in the gapless fluctuations of the internal degrees of freedom of the order parameter.

For small temperatures $t > 0.8$ the contribution from the electronic channels is negligible³⁰ and the quadratic temperature dependence of the non-linear sigma model Eq. (42) dominates the specific heat.

$$C_s|_{t \rightarrow 1} = 3 \frac{3 \zeta(2)}{\pi} \frac{T^2}{(v_\nu)^2} \approx 3.4 \frac{T^2}{(\bar{v}_{\text{eff}})^2} \quad (64)$$

Here $\zeta(n)$ is Riemann’s zeta function and the prefactor 3 is the multiplicity of the channels $\mu = s, f$ that contribute.¹⁰⁵ From the fit in Fig. 2 (dash-dotted line) one extracts $\bar{v}_{\text{eff}} \approx 22$ K. The resulting value of $s_0 \approx 4.7$ is only an order of magnitude estimate since the accurate prefactor in Eq. (48) is not known. If one assumes the magnetic channel to be gapped the numbers are $\bar{v}_{\text{eff}} \approx 38$ K and $s_0 \approx 2.7$.

The value of $2\bar{v}_{\text{eff}} \approx 44 - 76$ K must be compared with the quasi one-dimensional magnetic excitation velocity determined in Ref. 32 as $v_{\text{eff}} \sim 10^2$ K albeit outside the Fermi liquid regime. The discrepancy must be attributed to effects of the two-dimensional coupling and the pair correlations in the superconducting state. The fact that the numbers are of the same order of magnitude is a non-trivial consistency check of the theory.

The specific heat has been reproduced fairly well within the p -wave approach by different groups^{30,38,39} by modeling the gapless excitations via introduced line nodes or a two-gap scenario,⁴⁷ where one of the gaps is very small. Since a number of experimental probes require a rather homogeneous in-plane gap^{17,20,21,23} only horizontal line nodes are possible. The latter require the fine tuning of a number of parameters.^{38,47,106,39} The finite slope near T_c has not been addressed yet. It would

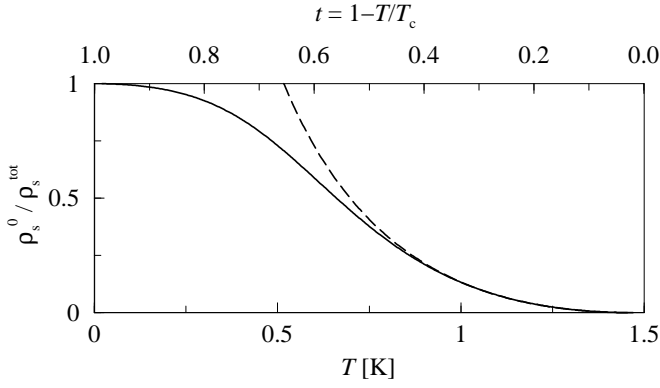


FIG. 3. Normalized Inverse stiffness $\rho_s^0/\rho_s^{\text{tot}}(T)$ (full line) from Eq. (65) for $\rho_s^0 \approx \bar{v}_{\text{eff}}$. The broken line shows the asymptotic part $\bar{v}_{\text{eff}}/\rho_s^{\text{amp}}$.

be interesting to repeat those approaches using the pairing potential in Eq. (4) including the gapless fluctuations of the internal degrees of freedom of the order parameter.

C. Stiffness and effective saddle-point regime

The stiffness near the phase transition, where the amplitude-Goldstone mode coupling is relevant, has been determined in Sec. III E 2 as $\rho_s^{\text{amp}} \approx \beta \langle X^2 \rangle A_\nu \approx T \frac{\bar{v}_{\text{eff}}^2}{\Delta^2}$. At low temperatures it has been determined within the non-linear sigma model Eq. (42) as $\rho_s^0 \sim \bar{P}^2 A_\nu |_{T \rightarrow 0}$. Since at low temperatures the exact relation between \bar{P} and the gap is not known [c.f. Eq. (40)] a precise numerical determination of ρ_s^0 is not possible. For sufficiently strong coupling the reasonable assumption is that the stiffness is of the order of the typical energy scale of the system, i.e., $\rho_s^0 \approx \bar{v}_{\text{eff}}$ (c.f. Ref. 43).

To obtain a qualitative picture of the temperature dependence of the stiffness the approximate interpolation formula

$$\rho_s^{\text{tot}}(T) \approx \sqrt{(\rho_s^0)^2 + (\rho_s^{\text{amp}})^2} \approx \bar{v}_{\text{eff}} \sqrt{1 + \frac{T^2 \bar{v}_{\text{eff}}^2}{\Delta^4}} \quad (65)$$

can be applied. The full line in Fig. 3 shows the normalized inverse stiffness from Eq. (65), the broken line is the asymptotic part $\bar{v}_{\text{eff}}/\rho_s^{\text{amp}}$. The temperature dependence of $\Delta(T)$ has been modeled via Eq. (60).

At intermediate temperatures $0.8 > t > 0.05$ the stiffness increases as $\sim t^{-2}$ and the integrals in the non-linear sigma models need to be cut off as in Eq. (47). For $t < 0.05$ one has $\bar{v}_{\text{eff}}/\rho_s^{\text{amp}} \leq 10^{-3}$ which is sufficiently small to justify the effective saddle point approach to the fluctuation action Eq. (48) and the resulting Landau expansion of the free energy Eq. (58).

For $t > 0.05$ the effective saddle point approximation Eq. (48) is not applicable any more. The third order term in Eq. (58) then is not present in that form anymore which enhances the importance of the higher order

terms in Eq. (63) and contributes to the rather sharp maximum of the specific heat. Note that even in BCS theory the specific heat is much more sensitive to the higher order terms that stem from the opening of the single particle gap than the temperature dependence of the order parameter itself.

D. Knight shift, static susceptibility, NQR, and universal thermal transport

The explanation of the observed absence of a change in the Knight shift¹⁴ and the magnetic susceptibility¹⁵ in the superconducting phase is trivial within the present model. All order parameter components carry spin one and thus no electronic magnetic moments are lost in the superconducting phase.

The relaxation times determined by NQR are consistent with gapless, two-dimensional fluctuations in the superconducting state.⁹ The qualitative agreement with the model presented here is obvious.

The thermal transport also is consistent with the presence of gapless fluctuations below T_c .³¹ The observed universal linear temperature dependence for $T \rightarrow 0$ is determined by the long wavelength excitations of the internal degrees of freedom of the order parameter and is consequently determined by the properties of collective state much rather than by the number of impurities in the system.

E. Order parameter symmetry

Equation (31) reveals the spatial order parameter anisotropy

$$\langle \mathbf{P} \rangle \propto \langle \Omega_f \rangle = \begin{pmatrix} \langle \sin(\sqrt{\pi}\phi_f - \sqrt{2}\bar{y}) \rangle \\ \langle \sin(\sqrt{\pi}\phi_f - \sqrt{2}\bar{x}) \rangle \end{pmatrix} \quad (66)$$

As discussed in Sec. III C the pair correlations for $\langle \Omega_{f,x} \rangle$ are larger along \bar{x} or [110] and for $\langle \Omega_{f,y} \rangle$ are larger along \bar{y} or $[\bar{1}10]$. The simplest parameterization is

$$\langle \Omega_f \rangle = \frac{\langle \Omega_{f,0} \rangle}{\sqrt{2}} \begin{pmatrix} 1 \\ 1 \end{pmatrix} + \sin 2\eta \frac{\langle \Omega_{f,1} \rangle}{\sqrt{2}} \begin{pmatrix} 1 \\ -1 \end{pmatrix}, \quad (67)$$

where the angle η is measured with respect to the [100] axis. Each component has a two-fold symmetry while the resulting spatial symmetry of the total order parameter reflects the four-fold axis of the underlying lattice.

$$|\langle \Omega_f \rangle| = \sqrt{\langle \Omega_{f,0} \rangle^2 + \langle \Omega_{f,1} \rangle^2 \sin^2 2\eta} \quad (68)$$

Oriented magnetic fields and temperature gradients break the SO(2) symmetry of Ω_f (Sec. III C) and reveal the two-fold symmetry of the components. Thermal conductivity measurements²¹ suggest that $\langle \Omega_{f,1} \rangle / \langle \Omega_{f,0} \rangle \approx$

0.02. A more careful analysis of the upper critical fields²³ in Ref. 41 yields $\langle\Omega_{f,1}\rangle/\langle\Omega_{f,0}\rangle = 0.034$ which leads to a spatial anisotropy of the order parameter components of 7%. The the four-fold symmetry of the total order parameter is then

$$|\langle\Omega_f\rangle| \approx \langle\Omega_{f,0}\rangle \left(1 + \frac{\langle\Omega_{f,1}\rangle^2}{\langle\Omega_{f,0}\rangle^2} \sin^2 2\eta \right), \quad (69)$$

which is also consistent with the experimental observations.²¹

The experimentally implied existence of two order parameter components with a slight spatial anisotropy⁷⁷ thus follows quite naturally out of the degenerate saddle points in the flavor channel discussed in Sec. III B.

V. RELATION TO THE p -WAVE APPROACH

A large number of experiments in superconducting samples of Sr₂RuO₄ have been interpreted in terms if the time reversal symmetry breaking p -wave state with symmetry E_u and order parameter $\mathbf{d}(\mathbf{k}) = \hat{z}(k_x \pm ik_y)$.^{53,6} As has been discussed throughout the manuscript most experimental results find alternative interpretations within the present approach. Examples are

(i) the observed density of states below the superconducting gap^{28–31,9} that has persistently been interpreted as an indication for line-nodes in the gap function while it may well originate from any kind of gapless, two-dimensional excitations with linear dispersion (Secs. III E, IV B, and IV D);

(ii) the c -axis pressure dependence of T_c that was interpreted in Ref. 49 as a consequence of a shift of the γ band closer to the van Hove singularities near the M point while in Sec. II it is viewed as the simple enhancement of the inter-plane coupling;

(iii) the strong in-plane coupling of strain to the superconductivity which was interpreted as a possible indication of an order parameter of the form $\mathbf{d}(\mathbf{k}) = \hat{z}(k_x \pm ik_y)$ while the anisotropy of the components of Ω_f can account for the same effect for symmetry reasons (Sec. III E);

(iv) the change in the μ SR relaxation rate across the superconducting phase transition that was interpreted as an indication for a time-reversal symmetry breaking pairing state^{16,53} while it may as well stem from the scattering of gapless magnetic excitations off the Muon spin (Sec. IV A);

(v) the sensitivity of the superconductivity to non-magnetic impurities which has been interpreted as an indication for higher angular momentum pairing states^{29,107,108} while it follows directly out of the symmetry of the orbital-singlet pairing state as discussed in Ref. 34.

These similarities between the approaches appear not very surprising when considering that the spin-flavor phase space discussed herein includes a time-reversal

pairing state similar to the p -wave E_u state. The flavor expectation values $\langle\Omega_f\rangle$ in Eq. (31) possibly contain contributions that are odd in real space, i.e., $\langle\sin\sqrt{2y}\cos\sqrt{\pi}\phi_f\rangle \neq 0$ and $\langle\sin\sqrt{2x}\cos\sqrt{\pi}\phi_f\rangle \neq 0$, and consequently a representation

$$\langle\Omega_p\rangle \propto \begin{pmatrix} \langle\sin\sqrt{2y}\cos\sqrt{\pi}\phi_f\rangle + i\langle\sin\sqrt{2x}\cos\sqrt{\pi}\phi_f\rangle \\ \langle\sin\sqrt{2y}\cos\sqrt{\pi}\phi_f\rangle - i\langle\sin\sqrt{2x}\cos\sqrt{\pi}\phi_f\rangle \end{pmatrix} \quad (70)$$

can be constructed with $\Omega_p \in \{\Omega_f \otimes \Omega_s\}$. The magnetic configuration of Ω_p depends on the details of the spin-flavor coupling terms and an easy-plane configuration as discussed in Sec. IV A and in Ref. 41 is quite conceivable. The present approach with mixed-orbital singlets can thus be generalized to include the p -wave^{76,77} E_u picture.

The conceptual advantage of the present approach is its derivation from a microscopic model. It allows to study interaction effects like the presence of two degenerate saddle points in detail—at least on a qualitative basis. Phenomenologically the important difference is that here Hund’s rule coupling is emphasized over effects from spin-orbit coupling as discussed in Sec. II A which allows for the degeneracy in the internal degrees of freedom (Sec. III E). This leads to a coherent description of a multitude of observations in Sr₂RuO₄ including the experiments discussed herein as well as the normal phase magnetism (Ref. 32), the interplay of the lattice symmetry, impurities and interaction effects (Ref. 34), and the magnetic field dependence (Ref. 41).

Resulting specific advantages over the p -wave E_u description are

(i) no need to construct horizontal line nodes or two-gap states which require parameter fine tuning and which have not been confirmed experimentally;

(ii) no inconsistency between the gap value extracted from Andreev reflection spectroscopy with respect to neutron scattering results (Sec. IV A);

(iii) the correct two-component order parameter symmetry as determined via thermal transport and upper critical field measurements (Sec. IV E);

(iv) the description of the temperature slope of the specific heat near T_c (Sec. IV B) as well as the magnetic field dependence of the specific heat near H_c (Ref. 41).

To obtain a more conclusive discrimination of the state promoted in this series of papers and the p -wave E_u state we propose to study a detailed Landau-Ginzburg functional¹⁰⁹ that contains in its parameter space the degenerate state described herein as well as the special case^{76,77} given in Eq. (70). Experimentally, the presence of the $\bar{\Omega}_f$ mode might be detectable via microwaves.

VI. CONCLUSIONS

From the approach discussed in the present paper the essential physical properties of the superconducting state

in Sr₂RuO₄ can be summarized as follows.

The body centered tetragonal structure gives rise to inter-plane pair correlations in the d_{yz} and d_{zx} orbitals enhanced by umklapp scattering processes. The superconducting order parameter is found to be a mixed-orbital-singlet spin-one-triplet. The bosonized description of the in-plane electron correlations is consistent with the order parameter and the slight easy plane configuration of the magnetic moments. The model reveals that the order parameter has two slightly anisotropic spatial components.

The absence of a change in the Knight shift and the magnetic susceptibility in the superconducting phase follows trivially from the spin-one Cooper pairs. The experimental thermal conductivity and upper critical fields are consistent with a spatial anisotropy of the order parameter components of 7%.

The different components of the order parameter in the spin and flavor sector give rise to two-dimensional gapless fluctuations. They are modeled by a 2+1 dimensional non-linear sigma model. Near the phase transition the two-dimensional gapless fluctuations account for the linear dependence of the pair density and the specific heat on the reduced temperature. At low temperatures they yield the quadratic temperature dependence of the specific heat, the cubed temperature dependence of the NQR relaxation time, and the universal linear temperature dependence of the thermal transport.

The finite pair density of the electrons in the d_{xy} orbitals is induced by the inter-band proximity effect. There is only one phase transition in the absence of magnetic fields and one single particle gap.

ACKNOWLEDGMENTS

I am grateful to V. J. Emery for initiating this project. I thank S. Carr, D. F. Agterberg, A. M. Tsvelik, M. Sgrist, B. O. Wells, J. Kroha, J. Brinckmann, M. Eschrig, K. Kikoin, H.-H. Klauss, M. Weinert, A. Klümper, and H. Keiter for instructive and stimulating discussions. I thank A. M. Tsvelik and G. E. Volovik for valuable comments on the spectra in triplet superconductors and ³He-A. The work was supported by DOE contract number DE-AC02-98CH10886 and the Center for Functional Nanostructures at the University of Karlsruhe.

APPENDIX: DERIVATIONS FOR THE ORDER PARAMETER FLUCTUATIONS

The expressions that are used in the manuscript to describe the fluctuations of the internal degrees of the order parameter can be derived within standard perturbative approaches.^{43,72,82–84,93} Within the vectorial representations introduced in Sec. IIIB the pair operators in the

relevant orbital-singlet spin-triplet channel are given as

$$\mathbf{P}_t^s = \frac{2}{\pi} \sin \sqrt{\pi} \phi_{sf} \boldsymbol{\Omega}_\rho \otimes \boldsymbol{\Omega}_s \otimes \boldsymbol{\Omega}_f. \quad (71)$$

Recall that the flavor degrees $\boldsymbol{\Omega}_f$ of freedom stem from the symmetry of the bosonized action which suggest a two-fold degenerate saddle point.

The superconducting state that is discussed in this paper involves the breaking of various continuous symmetries. The broken gauge symmetry is parameterized via the charge phase $\langle \boldsymbol{\Omega}_\rho \rangle$, the SO(3) symmetry of the magnetic moment of the spin-triplet Cooper pairs enters via $\langle \boldsymbol{\Omega}_s \rangle$, and the broken SO(2) symmetry of the flavor channel is given by $\langle \boldsymbol{\Omega}_f \rangle$. The expectation value of the order parameter is given in vectorial representation via

$$\langle \mathbf{P}_t^s \rangle = \bar{P} \bar{\boldsymbol{\Omega}}_\rho \otimes \bar{\boldsymbol{\Omega}}_s \otimes \bar{\boldsymbol{\Omega}}_f, \quad (72)$$

where \bar{P} is the order parameter amplitude as defined in Eq. (34) and $\bar{\boldsymbol{\Omega}}_\mu(\mathbf{r})$ are normalized according to Eq. (33). The phase of $\langle \sin \sqrt{\pi} \phi_{sf} \rangle$ can be absorbed in $\bar{\boldsymbol{\Omega}}_\rho$ via a gauge transformation.

The ground state is degenerate with respect to rotations of $\bar{\boldsymbol{\Omega}}_\mu$ giving rise to long wavelength gapless excitations—the Goldstone modes. In order to describe the dynamics of the system in the ordered phase it proves useful to introduce pair operators that are related to those in Eq. 71 by a shift of the pair expectation value, i.e., $\tilde{\mathbf{P}} \equiv \mathbf{P}_t^s - \langle \mathbf{P}_t^s \rangle$. The mean-field decoupling Eq. (15) then can be rewritten as the exact relation

$$\mathbf{P}_t^{s\dagger} \mathbf{P}_t^s = \mathbf{P}_t^{s\dagger} \langle \mathbf{P}_t^s \rangle + \mathbf{P}_t^s \langle \mathbf{P}_t^s \rangle^* - |\langle \mathbf{P}_t^s \rangle|^2 + \tilde{\mathbf{P}}^\dagger \tilde{\mathbf{P}}. \quad (73)$$

Using Eq. (73) the orbital-singlet spin-triplet part of the pair Hamiltonian Eq. (3) decouples into two parts $H_p = H_{mf} + H_{fl}$, where the mean-field part is given by Eq. (16) or, in its bosonized version, by Eq. (35). The fluctuation part is

$$H_{fl} = \sum_{\mathbf{q}} \frac{V_{\mathbf{q}}}{N} \tilde{\mathbf{P}}^\dagger(\mathbf{q}) \tilde{\mathbf{P}}(\mathbf{q}). \quad (74)$$

The partition function of the whole system can now be expressed via a standard perturbative approach^{110,83,84,43,55} as

$$Z = e^{-S_{mf}} \int \mathcal{D}[\mathbf{X}, \mathbf{X}^*] \exp\{-S_{fl}[\mathbf{X}, \mathbf{X}^*]\}. \quad (75)$$

The mean-field action is composed of Eqs. (39), (38), and (41) as $S_{mf} = S_s^{\text{eff}} + S_{sf}^{\text{eff}} + S_c$ and accounts for the physics contained in the saddle point including the mean-field temperature dependence of the gap and the Goldstone modes as discussed in Appendix A below. The thermodynamic averaging in the amplitude fluctuation part $\sim S_{fl}[\mathbf{X}, \mathbf{X}^*]$ is performed with respect to the mean-field system S_{mf} . The vectorial character of the pair operators leads to Hubbard-Stratonovich fields^{83,84,43} \mathbf{X} and

\mathbf{X}^* which also have vectorial character and can be parameterized as

$$\mathbf{X} = X \bar{\Omega}_\rho \otimes \bar{\Omega}_s \otimes \bar{\Omega}_f. \quad (76)$$

The integral measure contains the averaging over the angular components of the Hubbard-Stratonovich fields^{83,84,43}

$$\mathcal{D}[\mathbf{X}, \mathbf{X}^*] = \prod_{\mathbf{q}, \omega_n} \sqrt{\beta |V_{\mathbf{q}}|} \frac{dX_{\mathbf{q},n}}{\pi} \frac{d\bar{\Omega}_\rho}{2\pi} \frac{d\bar{\Omega}_s}{4\pi} \frac{d\bar{\Omega}_f}{2\pi}. \quad (77)$$

The ω_n are bosonic Matsubara frequencies. The averaging over the angular components corresponds to an averaging over the degenerate ground states of the system.^{83,84}

A. Goldstone modes

In the present approach the Goldstone modes that correspond to the broken local spin rotational, flavor, and gauge invariance are implicitly contained in the mean-field system defined by the actions $S_{\text{mf}} = S_s^{\text{eff}} + S_{\text{sf}}^{\text{eff}} + S_c$. This becomes obvious when considering that the mass terms in Eqs. (39), (38), and (41) are decreased when the operator Ω_μ is not parallel to the mean direction $\bar{\Omega}_\mu$. A direct derivation of the non-linear sigma model in Eq. (42) that describes the dynamics of the Goldstone modes within the present approach would require non-Abelian bosonization in order to maintain the symmetry of the Hamiltonian explicitly.^{71,72} In the light of the well established results in the literature the involved explicit derivation herein appears obsolete.

A simple qualitative argument that makes the underlying physics transparent to the reader shall be discussed instead. The finite local angle $\eta_\mu(\mathbf{r}, \tau) = \angle[\Omega_\mu(\mathbf{r}, \tau), \bar{\Omega}_\mu(\mathbf{r}, \tau)]$ increases the energy⁶³ of the system since the mass term determining the gap is lowered. Consequently there is a restoring force which can be assumed linear in $\eta_\mu(\mathbf{r}, \tau)$ if the angle is sufficiently small. Small fluctuations of $\eta_\mu(\mathbf{r}, \tau)$ are consequently expected to be harmonic. Their spectrum is gapless since the restoring force vanishes for $\eta_\mu(\mathbf{r}, \tau) = 0$. The excitation velocity should be of the same order^{83,84,111} as the velocity of the gapped amplitude mode (Appendix B). Finally, the local constraint of $|\bar{\Omega}_\mu(\mathbf{r}, \tau)|^2 = 1$ distinguishes the angular fluctuations from other harmonic systems and leads to the effective description via the non-linear sigma models given by Eq. (42) in Sec. III E.

At sufficiently small temperatures and energy scales $T, \omega \ll \Delta$ the stiffness of the non-linear sigma model describing the angular fluctuations has been determined^{71,72} to scale with the square of the order parameter amplitude $\sim \bar{P}^2$, albeit with corrections^{84,43} that depend on the specific correlations of the system. As will be discussed in Appendix B2 the gap in the ordered phase plays the role of a cutoff.⁷¹ This cutoff becomes

small as the gap becomes small and has important physical implications.¹¹²

B. Gaussian amplitude fluctuations

The integral term in Eq. (75) contains the fluctuations $\tilde{\mathbf{P}}$ of the system involving changes in amplitude of the order parameter. The amplitude fluctuation part is expanded up to second order^{83,84} in the complex fields \mathbf{X} and \mathbf{X}^* . Considering that per definition $\langle \tilde{\mathbf{P}} \rangle = 0$ one has

$$S_{\text{fl}}[\mathbf{X}, \mathbf{X}^*] = \beta \sum_{\mathbf{q}, \omega_n} |V_{\mathbf{q}}| \left[1 - |V_{\mathbf{q}}| \chi_{2,\pm}^{(P)}(\mathbf{q}, i\omega_n) \right] |\mathbf{X}(\mathbf{q}, i\omega_n)|^2. \quad (78)$$

For the relevant umklapp scattering near $\mathbf{q} \sim 0$ the potential has been set $V_{\mathbf{q}} \approx -|V_{\mathbf{q}}|$. The pair correlation function $\chi_{2,\pm}^{(P)}$ needs to be calculated with respect to S_{mf} . Since S_{mf} describes a gapped system in the ordered phase $\chi_{2,\pm}^{(P)}(0, 0)|_{T < T_c} < \chi_{2,\pm}^{(P)}(0, 0)|_{T = T_c}$ and the action in Eq. (78) is stable.

Limiting the description to the low energy long wavelength properties one may expand

$$|V_{\mathbf{q}}|^2 \chi_{2,\pm}^{(P)}(\mathbf{q}, \omega_n) \approx |V_0|^2 \chi_{2,\pm}^{(P)}(0, 0) + A_x q_x^2 + A_y q_y^2 + \left(\frac{A_x}{(av_x)^2} + \frac{A_y}{(av_y)^2} \right) (i\omega_n)^2, \quad (79)$$

where A_ν and v_ν are defined after analytical continuation $i\omega_n \leftrightarrow \lim_{\epsilon \rightarrow 0} (\omega + i\epsilon)$ in Eqs. (43) and (44), respectively. As discussed in Sec. III E 1 one can assume for the low temperature and low energy regime the system to be isotropic in the x - y plane with $A_\nu = A_x = A_y$ and $v_\nu = v_x = v_y$.

Using Eq. (79) and transforming Eq. (78) to Euclidean space representation the action becomes

$$S_{\text{fl}} = \int_{-L}^L d^2r \int_0^\beta d\tau |V_0| \left[1 - |V_0| \chi_{2,\pm}^{(P)}(0, 0) \right] X^2 + \int_{-L}^L d^2r \int_0^\beta d\tau \sum_{\nu=x,y} A_\nu \left[\frac{|\partial_\tau \mathbf{X}|^2}{(av_\nu)^2} + |\partial_\nu \mathbf{X}|^2 \right]. \quad (80)$$

The \mathbf{q} dependence of the term linear in $|V_{\mathbf{q}}|$ has been neglected. Note that in Euclidean space $|\mathbf{X}|^2 \equiv X^2$ because of the local constraints $|\bar{\Omega}_\mu(\mathbf{r}, \tau)|^2 \equiv 1$. Another important consequence of the local constraint is that $\Omega_\mu \partial_\tau \Omega_\mu = \Omega_\mu \partial_\nu \Omega_\mu = 0$. Consequently angular and amplitude contributions to the derivatives in Eq. (80) decouple for $\nu = x, y, \tau$ as

$$|\partial_\nu \mathbf{X}|^2 = (\partial_\nu X)^2 + X^2 \sum_{\mu=\rho,s,f} (\partial_\nu \bar{\Omega}_\mu)^2. \quad (81)$$

Now the different modes around the saddle point can be discussed in detail.

1. Amplitude mode

The part of Eq. (80) that describes the amplitude excitations is in Fourier space

$$S_{\text{amp}}[X, X^*] = \beta \sum_{\mathbf{q}, \omega_n} \left[|V_0| \left(1 - |V_0| \chi_{2,\pm}^{(P)}(0, 0) \right) + \sum_{\nu=x,y} A_\nu \left((aq_\nu)^2 + \frac{(i\omega_n)^2}{v_\nu^2} \right) \right] |X(\mathbf{q}, i\omega_n)|^2 \quad (82)$$

and describes Gaussian fluctuations around the static saddle point.

In order for the action Eq. (82) to be consistent with the mean-field pair correlation function estimated by Eq. (45) one must require that

$$\beta \langle X(\mathbf{q}, i\omega_n) X(-\mathbf{q}, -i\omega_n) \rangle = \chi_{\text{BCS}}^{(P)}(\mathbf{q}, i\omega_n). \quad (83)$$

After analytical continuation $i\omega_n \leftrightarrow \lim_{\epsilon \rightarrow 0} (\omega + i\epsilon)$ and comparing Eqs. (82), (83), and $\chi_{\text{BCS}}^{(P)}$ in Eq. (45) one can identify

$$A_\nu \approx \frac{\bar{v}_{\text{eff}}^2}{\Delta f_0}, \quad (84)$$

$$v_\nu \approx \bar{v}_{\text{eff}}, \quad (85)$$

as well as

$$|V_0| \left(1 - |V_0| \chi_{2,\pm}^{(P)}(0, 0) \right) \approx \frac{\Delta}{f_0}. \quad (86)$$

The \mathbf{q} dependence of $f(\mathbf{q}) \approx f(0) \equiv f_0$ has been neglected. The dispersion of the amplitude mode then can readily be read off from Eq. (82) as

$$\omega_{\text{amp}} = \bar{v}_{\text{eff}} \sqrt{a^2 \mathbf{q}^2 - \Delta^2 / \bar{v}_{\text{eff}}^2} \quad (87)$$

and has the desired shape with an excitation gap Δ underlining the self-consistency of the approach.

The identical self-consistent results are obtained by directly identifying

$$|V_{\mathbf{q}}|^{-1} \left[1 - |V_{\mathbf{q}}| \chi_{2,\pm}^{(P)}(\mathbf{q}, i\omega_n) \right]^{-1} \approx \chi_{\text{BCS}}^{(P)}(\mathbf{q}, i\omega_n) \quad (88)$$

in the action Eq. (78) which again shows the stability of the latter since $\chi_{\text{BCS}}^{(P)}(0, 0) > 0$.

2. Amplitude-Goldstone mode coupling

Starting from the fluctuation action Eq. (80), including the identity Eq. (81), using the identifications Eqs. (84) and (85), and transforming to Fourier space the action

$$S_{\Omega}^{\text{amp}}[\mathbf{\Omega}_\mu, \mathbf{\Omega}_\mu^*] = \beta \sum_{\mathbf{q}, \omega_n} \sum_{\nu=x,y} A_\nu \sum_{\mu=\rho,s,f} X^2(\mathbf{q}, i\omega_n) \times \left((aq_\nu)^2 + \frac{(i\omega_n)^2}{v_\nu^2} \right) |\mathbf{\Omega}_\mu(\mathbf{q}, i\omega_n)|^2 \quad (89)$$

is obtained for the angular modes. Except for the prefactors it is equivalent to the non-linear sigma model Eq. (42) used to describe the low temperature, low energy excitations of the angular Goldstone modes [Appendix A, Sec. III E].

The action Eq. (89) is the lowest order amplitude-Goldstone mode coupling term. This becomes evident when replacing the amplitude of the pair fluctuation field X by its expectation value, i.e., $X \rightarrow \langle X \rangle = 0$: in the absence of amplitude fluctuations Eq. (89) does not contribute. This is reminiscent of the decoupling of the pair operators into angular and amplitude parts through Eq. (73) where the angular fluctuations that give rise to the Goldstone modes have been included in the mean-field action S_{mf} [Appendix A].

In a rigorous approach the amplitude fluctuations have to be integrated out⁹³ in order to determine the contribution of the action Eq. (89) to the free energy of the system. In the light of the *local* constraint $|\mathbf{\Omega}_\mu(\mathbf{r}, \tau)|^2 = 1$ the treatment of the resulting terms is not evident. Instead, on the mean-field level one can estimate the impact of the amplitude-Goldstone mode coupling by replacing the square of the amplitude fields by their expectation value, i.e., $\beta X^2(\mathbf{q}, i\omega_n) \rightarrow \beta \langle X^2(\mathbf{q}, i\omega_n) \rangle = \chi_{\text{BCS}}^{(P)}(\mathbf{q}, i\omega_n)$, in Eq. (89).

$\chi_{\text{BCS}}^{(P)}$ is given in Eq. (45) and diverges for $\omega^2 - v_\nu^2 \mathbf{q}^2 \rightarrow \Delta^2$. Consequently the excitation gap Δ indeed marks the ultraviolet cutoff discussed in the literature.^{71,72} Given the mean-field relation between the excitation gap and the coherence length $\Delta / \bar{v}_{\text{eff}} \approx \xi_{\text{BCS}}^{-1}$ the cutoff translates into a short range or large wavevector cutoff $a|\mathbf{q}| < \Delta / v_\nu$ in strict analogy to the discussion by Schulz⁴³ for the magnetic order in the repulsive Hubbard model.

For sufficiently low temperatures $T \ll \Delta$ the thermal occupation of states near the cutoff energy can be neglected and the gapless excitations are well described via the non-linear sigma models given by Eq. (42) in Sec. III E. Since in this case the amplitude mode has a large gap compared with temperature, contributions from the amplitude mode and the amplitude-Goldstone mode coupling term are negligible.

Closer to the phase transition corrections from Gaussian fluctuations become relevant⁹³ and the energy and wavevector cutoff will play a crucial role and needs to be included in the action Eq. (89). In continuum representation for the momenta this leads to Eq. (47) in Sec. III E 2.

Note that for small energies and wavevectors the ω and \mathbf{q} dependence of $\chi_{\text{BCS}}^{(P)}(\mathbf{q}, i\omega_n) \sim \chi_{\text{BCS}}^{(P)}(0, 0) = f_0/\Delta$ and $|\Omega_\mu(\mathbf{q}, i\omega_n)|^2 \sim |\Omega_\mu|^2$ is not expected to alter the physical result and consequently have been neglected in Eq. (47).

3. Limits of the applicability

It is well known⁹³ that in the critical region around the phase transition the Gaussian approximation for fluctuation corrections as derived in Appendix B breaks down. The contributions are divergent and higher order terms have to be included in a non-perturbative fashion. The critical region can be estimated by the rounding of the measured specific heat near the phase transition (Fig. 2 in Sec. IV B) and yields a temperature interval of $T_c \pm 0.02$ K. The results herein including Eq. (58) are only applicable for $T \leq T_c - 0.02$ K or for reduced temperatures $|t| \geq 0.01$. Note that within the framework of the third order phase transition considered in Sec. IV B the determination of T_c and thus of the critical region differs from the usual “mid transition point” estimate.

The possible impact^{55,87,88} of additional topological terms is addressed in Sec. III E.

¹ Y. Maeno *et al.*, Nature (London) **372**, 532 (1994).

² M. Braden *et al.*, Phys. Rev. B **57**, 1236 (1998).

³ T. Oguchi, Phys. Rev. B **51**, 1385 (1995).

⁴ A. P. Mackenzie *et al.*, Phys. Rev. Lett. **76**, 3786 (1996).

⁵ M. Schmidt *et al.*, Phys. Rev. B **53**, R14761 (1996).

⁶ Y. Maeno, T. M. Rice, and M. Sigrist, Physics Today **54**, 42 (2001).

⁷ Y. Maeno *et al.*, J. Phys. Soc. Jpn. **66**, 1405 (1997).

⁸ A. P. Mackenzie *et al.*, J. Phys. Soc. Jpn. **67**, 385 (1998).

⁹ K. Ishida *et al.*, Phys. Rev. Lett. **84**, 5387 (2000).

¹⁰ A. V. Puchkov, Z.-X. Shen, T. Kimura, and Y. Tokura, Phys. Rev. B **58**, R13322 (1998).

¹¹ T. M. Rice and M. Sigrist, J. Phys.: Condens. Matter **7**, L643 (1995).

¹² G. Baskaran, Physica B **223-224**, 490 (1996).

¹³ K. Ishida *et al.*, Phys. Rev. B **56**, R505 (1997).

¹⁴ K. Ishida *et al.*, Nature (London) **396**, 658 (1998).

¹⁵ J. A. Duffy *et al.*, Phys. Rev. Lett. **85**, 5412 (2000).

¹⁶ G. M. Luke *et al.*, Nature (London) **394**, 558 (1998).

¹⁷ F. Laube *et al.*, Phys. Rev. Lett. **84**, 1595 (2000).

¹⁸ Z. Q. Mao *et al.*, Phys. Rev. Lett. **87**, 037003 (2001).

¹⁹ M. A. Tanatar *et al.*, Phys. Rev. B **63**, 064505 (2001).

²⁰ M. A. Tanatar *et al.*, Phys. Rev. Lett. **86**, 2649 (2001).

²¹ K. Izawa *et al.*, Phys. Rev. Lett. **86**, 2653 (2001).

²² M. Suzuki *et al.*, J. Phys.: Condens. Matter **14**, 7371 (2002).

²³ H. Yaguchi *et al.*, submitted to Phys. Rev. B (2002), cond-mat/0106491.

²⁴ Y. Sidis *et al.*, Phys. Rev. Lett. **83**, 3320 (1999).

²⁵ A. Damascelli *et al.*, Phys. Rev. Lett. **85**, 5194 (2000).

²⁶ K. M. Shen *et al.*, Phys. Rev. B **64**, 180502(R) (2001).

²⁷ I. I. Mazin, D. A. Papaconstantopoulos, and D. J. Singh, Phys. Rev. B **61**, 5223 (2000).

²⁸ S. Nishizaki, Y. Maeno, and S. Farner, J. Phys. Soc. Jpn. **67**, 560 (1998).

²⁹ S. Nishizaki, Y. Maeno, and Z. Q. Mao, J. Low Temp. Phys. **117**, 1581 (1999).

³⁰ S. Nishizaki, Y. Maeno, and Z. Q. Mao, J. Phys. Soc. Jpn. **69**, 572 (2000).

³¹ M. Suzuki *et al.*, Phys. Rev. Lett. **88**, 227004 (2002).

³² R. Werner and V. J. Emery, cond-mat/0208306 (2002).

³³ R. Werner, cond-mat/0201293 (2002).

³⁴ R. Werner, cond-mat/0208301 (2002).

³⁵ M. Braden *et al.*, cond-mat/0206304 (2002).

³⁶ C. Bergemann *et al.*, Phys. Rev. Lett. **84**, 2662 (2000).

³⁷ C. Bergemann *et al.*, submitted to Adv. Phys. (2002).

³⁸ M. E. Zhitomirsky and T. M. Rice, Phys. Rev. Lett. **87**, 057001 (2001).

³⁹ J. F. Annett, G. Litak, B. L. Györfy, and K. I. Wysokiński, Phys. Rev. B in press (2002), cond-mat/0109023.

⁴⁰ F. H. L. Essler, A. M. Tsvelik, and G. Delfino, Phys. Rev. B **56**, 11001 (1997).

⁴¹ R. Werner, cond-mat/0208308 (2002).

⁴² H. J. Schulz, G. Cuniberti, and P. Pieri, cond-mat/9807366 (1998), lecture notes, Chai Laguna summer school 1997.

⁴³ H. J. Schulz, in *The Hubbard model: its physics and mathematical physics*, edited by D. Baerisvyl (Plemun, New York, 1995), p. 89, cond-mat/9402103.

⁴⁴ N. D. Mermin and H. Wagner, Phys. Rev. Lett. **17**, 1133 (1966).

⁴⁵ D. F. Agterberg, T. M. Rice, and M. Sigrist, Phys. Rev. Lett. **78**, 3374 (1997).

⁴⁶ I. Eremin, D. Manske, C. Joas, and K. H. Bennemann, Europhys. Lett. **58**, 871 (2002).

⁴⁷ H. Kusunose and M. Sigrist, cond-mat/0205050 (2002).

⁴⁸ A. A. Ovchinnikov and M. Y. Ovchinnikova, cond-mat/0205529 (2002).

⁴⁹ N. Okuda *et al.*, J. Phys. Soc. Jpn. **71**, 1134 (2002).

⁵⁰ N. Shirakawa *et al.*, Phys. Rev. B **56**, 7890 (1997).

⁵¹ R. Werner, *The spin-Peierls transition in CuGeO₃* (Ph.D. thesis, Dortmund, 1999), <http://eldorado.uni-dortmund.de:8080/FB2/l88/forschung/1999/werner>.

⁵² For the standard notation of the spin-triplet order parameter components see Refs. 34,55 or G. E. Volovik and L. P. Gor'kov, Sov. Phys. JETP Lett. **39**, 674 (1984).

⁵³ M. Sigrist *et al.*, Physica C **317-318**, 134 (1999).

⁵⁴ G. E. Volovik and M. V. Khazan, Sov. Phys. JETP **58**, 551 (1983).

⁵⁵ G. E. Volovik, *Exotic properties of superfluid ³He, Series in Condensed Matter Physics, Vol.1* (World Scientific, Singapore, 1992).

⁵⁶ E. Langmann and M. Wallin, Phys. Rev. B **55**, 9439 (1997).

⁵⁷ T. Takimoto, Phys. Rev. B **62**, R14641 (2000).

⁵⁸ R. J. Cava *et al.*, Phys. Rev. B **49**, 11890 (1994).

⁵⁹ A. Liebsch and A. Lichtenstein, Phys. Rev. Lett. **84**, 1591

- (2000).
- ⁶⁰ K.-K. Ng and M. Sigrist, J. Phys. Soc. Jpn. **69**, 3764 (2000).
- ⁶¹ J. E. Hirsch, Science **295**, 2226 (2002), cond-mat/0207371.
- ⁶² E. W. Carlson, V. J. Emery, S. A. Kivelson, and D. Orgad, in *The Physics of Conventional and Unconventional Superconductors*, edited by K. H. Bennemann and J. B. Ketterson (Springer, to appear, 2002), cond-mat/0206217.
- ⁶³ S. Lukyanov and A. Zamolodchikov, Nucl. Phys. B **493**, 571 (1997).
- ⁶⁴ V. J. Emery, in *Highly conducting one-dimensional solids*, edited by J. T. Devreese, R. P. Evrard, and V. E. van Doren (Plenum, New York, 1979), p. 247.
- ⁶⁵ D. Sénéchal, cond-mat/9908262 (1999).
- ⁶⁶ S. T. Carr and A. M. Tsvelik, Phys. Rev. B **65**, 195121 (2002).
- ⁶⁷ R. Mukhopadhyay, C. L. Kane, and T. C. Lubensky, Phys. Rev. B **64**, 45120 (2001).
- ⁶⁸ K. Kikoin, I. Kuzmenko, S. Gredeskul, and Y. Avishai, cond-mat/0205120 (2002).
- ⁶⁹ A. Luther and V. J. Emery, Phys. Rev. Lett. **33**, 589 (1974).
- ⁷⁰ A. Luther, Phys. Rev. B **15**, 403 (1977).
- ⁷¹ A. M. Tsvelik, *Quantum field theory in condensed matter physics* (Cambridge University Press, Cambridge, 1995).
- ⁷² A. O. Gogolin, A. A. Nersesyan, and A. M. Tsvelik, *Bosonization and strongly correlated systems* (Cambridge University Press, Cambridge, 1998).
- ⁷³ R. J. Baxter, *Exactly Solved Models in Statistical Mechanics* (Academic Press, London, 1982).
- ⁷⁴ A gap in all channels μ is also obtained when simply adding the mean-field term H_{mf} Eq. (16) to the high temperature Hamiltonians Eq. (19).
- ⁷⁵ P. W. Anderson, Phys. Rev. **112**, 1900 (1958).
- ⁷⁶ M. Sigrist, J. Phys. Soc. Jpn. **69**, 1290 (2000).
- ⁷⁷ D. F. Agterberg, Phys. Rev. B **64**, 052502 (2001).
- ⁷⁸ M. Tinkham, *Introduction to superconductivity, 2nd edition* (McGraw-Hill, New York, 1996).
- ⁷⁹ M. Sigrist and H. Monien, J. Phys. Soc. Jpn. **70**, 2409 (2001).
- ⁸⁰ Here the polar angle has been set $\theta_z = \pi/2$. A description for general θ_z within the framework of the bosonized model is not possible since $\theta_z = \pi/2 \rightarrow 0$ involves a dual transformation of the spin and spin-flavor fields.
- ⁸¹ S. Coleman, Phys. Rev. D **11**, 2088 (1975).
- ⁸² E. F. Fradkin, *Field Theories of Condensed Matter Systems* (Addison-Wesley, New York, 1991).
- ⁸³ H. J. Schulz, Phys. Rev. Lett. **65**, 2462 (1990).
- ⁸⁴ Z. Y. Weng, C. S. Ting, and T. K. Lee, Phys. Rev. B **43**, 3790 (1991).
- ⁸⁵ T. Akima, S. Nishizaki, and Y. Maeno, J. Phys. Soc. Jpn. **68**, 694 (1999).
- ⁸⁶ E. Babaev, Phys. Rev. Lett. **88**, 177002 (2002).
- ⁸⁷ In $^3\text{He-A}$ the presence of spin-orbit coupling yields a gap in the magnetic spectrum given by the Leggett frequency^{54,55} $\Omega_A^2 \approx a^2 \bar{v}_{\text{eff}}^2 / \xi_P^2$. The analogy here is the spin-flavor coupling. An estimate is obtained via $\xi_P/a \sim 250$ [K. Yoshida, Y. Maeno, S. Nishizaki, and T. Fujita, Physica C **80**, 161 (1996); A.P. Mackenzie *et al.*, Phys. Rev. Lett. **80**, 161 (1998)] and $\bar{v}_{\text{eff}} \sim 22$ K [Sec. IV B] as $\Omega_A < 0.1$ K which is negligible in the temperature range usually observed. A value of $\Omega_A \sim 0.08$ K is estimated in Ref. 41.
- ⁸⁸ Possible low energy contributions with quadratic dispersion^{54,55} are of the order $\Delta^2/v_F \sim 10^{-4}$ K and are negligible [$\Delta \sim 1$ meV, Sec. IV A].
- ⁸⁹ E. Rzepniewski *et al.*, cond-mat/0201032 (2002).
- ⁹⁰ J. M. Blatt, *Theory of superconductivity* (Academic Press, New York, 1964).
- ⁹¹ A. Luther and I. Peschel, Phys. Rev. B **12**, 3908 (1975).
- ⁹² G. S. Uhrig and H. J. Schulz, PRB **54**, R9624 (1996).
- ⁹³ A. Larkin and A.A. Varlamov, in *The Physics of Conventional and Unconventional Superconductors*, edited by K. H. Bennemann and J. B. Ketterson (Springer, to appear, 2002), cond-mat/0109177.
- ⁹⁴ L. D. Landau and E. M. Lifschitz, *Statistical Mechanics* (Pergamon Press, Oxford, 1988).
- ⁹⁵ A. Leclair and G. Mussardo, Nucl. Phys. B **552**, 624 (1999).
- ⁹⁶ A. Klümper, R. Raupach, and F. Schönfeld, Phys. Rev. B **59**, 3612 (1999).
- ⁹⁷ A. B. Zamolodchikov, Int. J. Mod. Phys. A **10**, 1125 (1995).
- ⁹⁸ S. Coleman, Ann. Phys. (N.Y.) **101**, 239 (1976).
- ⁹⁹ M. C. Cross and D. S. Fisher, Phys. Rev. B **19**, 402 (1979).
- ¹⁰⁰ F. D. M. Haldane, Phys. Rev. B **25**, 4925 (1982).
- ¹⁰¹ P. Ehrenfest, Comm. Phys. Lab. Univ. Leiden Suppl. **75b**, I,1 (1933).
- ¹⁰² C. P. Slichter, *Principles of magnetic resonance* (Springer, Berlin, 1990).
- ¹⁰³ G. E. Blonder, M. Tinkham, and T. M. Klapwijk, Phys. Rev. B **25**, 4515 (1982).
- ¹⁰⁴ K. Sengupta, H.-J. Kwon, and V. M. Yakovenko, Phys. Rev. B **65**, 104504 (2002).
- ¹⁰⁵ The SO(3) non-linear sigma model accounts for two degenerate transversal magnon modes.
- ¹⁰⁶ C. Honerkamp and M. Salmhofer, Phys. Rev. Lett. **87**, 187004 (2001).
- ¹⁰⁷ A. P. Mackenzie *et al.*, Phys. Rev. Lett. **80**, 161 (1998).
- ¹⁰⁸ Z. Mao, Y. Mori, and Y. Maeno, Phys. Rev. B **60**, 610 (1999).
- ¹⁰⁹ A. P. Protogenov, cond-mat/0205133 (2002).
- ¹¹⁰ J. W. Negele and H. Orland, *Quantum Many-Particle Systems* (Addison-Wesley, New York, 1988).
- ¹¹¹ J. R. Schrieffer, X. G. Wen, and S. C. Zhang, Phys. Rev. B **39**, 11663 (1989).
- ¹¹² S. Chakravarty, B. I. Halperin, and D. R. Nelson, Phys. Rev. B **39**, 2344 (1989).